JUNE 1970 MDC G1697

THERMIONIC ENERGY CONVERSION SYSTEM DESIGN

PHASE I - TECHNICAL INTERIM REPORT

Prepared Under Contract No. 952781 by
Donald W. Douglas Laboratories
McDonnell Douglas Astronautics Company — Western Division
Richland, Washington
for
JET PROPULSION LABORATORY

JUNE 1970 MDC G1697

THERMIONIC ENERGY CONVERSION SYSTEM DESIGN

PHASE I - TECHNICAL INTERIM REPORT

by
J. G. DeSteese

This work was performed for the Jet Propulsion Laboratory, California Institute of Technology, as sponsored by the National Aeronautics and Space Administration under Contract NAS7-100.

Prepared Under Contract No. 952781 by
Donald W. Douglas Laboratories
McDonnell Douglas Astronautics Company – Western Division
Richland, Washington
for
JET PROPULSION LABORATORY

PRECEDING PAGES BLANK NOT FILMED.

CONTENTS

FIGURES

SYMBOLS

A	=	Emitter area (cm^2)
d	=	Electrode spacing (mils)
e	=	Electronic charge (1.6×10^{-19} coulomb)
ℓ/a	=	Emitter lead length-to-area ratio
L/D	=	Cylindrical converter capsule length-to-diameter ratio
L_a/D_a	=	Aeroshell length-to-diameter ratio
P	=	Converter power (w_e)
$Parameter_o$	=	Optimum value of parameter (subscript)
P_g	=	Generator power (w_e)
P_{max}	=	Maximum converter power (w_e)
Q	=	Input thermal power (w_t)
Q_c	=	Sum of conduction components of thermal energy balance (w_t)
Q_e	=	Electron-cooling component of thermal energy balance (w_t)
Q_r	=	Radiation component of thermal energy balance (w_t)
R_L	=	Converter load resistance (Ω)
T	=	Surface temperature (°K)
T_c	=	Collector temperature (°K)
T_e	=	Emitter temperature (°K)
T_R	=	Temperature of liquid cesium reservoir (°K)
T_{rad}	=	Aeroshell heat rejection temperature (°K)
V_c	=	Converter electrode potential (v)
V_g	=	Generator voltage (v)
β	=	Aeroshell ballistic coefficient (lb/ft^2)
ϵ	=	Electrode emissivity
ϕ	=	Surface work function (ev)
ϕ_B	=	Electrode cesium-bare work function (ev)
ϕ_c	=	Collector work function (ev)
ϕ'_c	=	Collector emission barrier height (ev)
ϕ_e	=	Emitter work function (ev)
ϕ_{min}	=	Work function minimum on Rasor-Warner plot (ev)
ϕ_n	=	Neutralization work function (ev)

PRECEDING PAGE BLANK NOT FILMED.

SUMMARY

A novel and attractive radionuclide-powered thermionic conversion system is described which provides a highly flexible and redundant modular design approach to satisfy space power requirements up to several hundred watts. Current technology performance characteristics and growth potential have been calculated parametrically for 50, 100, and 200 w_e generators composed of multicell arrays of Isomite* converters. The choice and influence of thermionic parameters, emitter geometry, fuel form, helium management, array reliability, system integration, and nuclear safety requirements are considered. Plutonia-fueled multicell generators in this power range achieve a fully system-integrated specific power of 4 w_e/lb and conversion efficiencies in excess of 6.5%. High thermal power density heat sources (such as Cm-244 fuel forms) and near-future technology materials development would allow system specific power up to approximately 17 w_e/lb and efficiencies approaching 10%.

Isomite converters are self-contained, radionuclide-fueled-thermionic battery cells operating in a low-current-density, quasi-vacuum mode at temperatures (<1400°K) typical of thermoelectric devices. The multicell generator composed of 1 to 7 w_e converter module arrays, is not subject to application limitations imposed by the high-temperature (>1600°K) operational mode of conventional, high-current density thermionic devices. Isomite devices operate, however, with heat rejection temperatures (700° to 900°K) characteristic of most thermionic systems. The multicell generator is, therefore, an attractive power source for long-duration space missions and is probably the only candidate for missions requiring operation in high-temperature environments.

The modular "building-block" approach to generator design is shown to be valid over a wide range of power, with the advantage that a large number of generator configurations are available at low cost, following initial development and qualification of a single converter module.

*Isomite is a trademark name, the property of the McDonnell Douglas Corporation.

Results of this analysis show the most attractive current technology multicell system performance results with a plutonia-fueled array of basic 5 w_e converter modules in aeroshell structures of conventional design. It is recommended that the Phase II effort establish a 100 w_e generator design based on this module power incorporating credible near-term technology and construction techniques.

Technical Monitor on this program for the Jet Propulsion Laboratory is Peter Rouklove.

Section 1
INTRODUCTION

This informal Interim Technical Report is deliverable under Article 1(a) 3(B) of Contract 952781 and summarizes Phase I of a system design study to identify the parametric performance characteristics of three multicell generators in the power range from 50 to 200 w_e. This report when approved by JPL provides the basis for the Phase I section of the Final Technical Report.

The direction taken by thermionic research and development in the early 1960's concentrated on cesium plasma devices operating with high emitter temperatures (>1600°K). Radionuclide-thermionic electric power sources can be classified according to the mode of heat transfer between heat source and converter. Typical configurations involve thermal coupling by direct conduction (Reference 1), fluid-metal loops (Reference 2), and radiant energy (Reference 3). Although components of several space power generator concepts have been developed using conventional converters powered by radionuclide thermal sources, the thermoelectric generator (RTG) has been favored for most applications to date, despite the projected superior specific power and competitive efficiency of thermionic systems. The reasons for this preference and consequent low level of interest in thermionic generators have been that relatively short demonstrated life, stringent requirements for high temperature fuel and materials technology, and low reliability are considered inherent characteristics high temperature thermionic devices.

In the last three years, the McDonnell Douglas Corporation has developed a novel, quasi-vacuum mode thermionic radionuclide battery cell operating at low emitter temperatures (<1400°K). Attractive features resulting from low temperature operation include efficient small module design, direct thermal coupling to fuels of any practical thermal power density, inherently compatible materials, and long life. The vacuum-mode thermionic converter retains the high temperature heat rejection capability (700° to 900°K) of conventional thermionic converters.

Although RTG's have an established position in space power applications, based on their current level of development and demonstrated reliability, their characteristically low heat rejection temperatures are unsuitable for high-temperature operational environments (Venus Lander vehicle, near-sun, and Mercury missions). The performance of other interplanetary vehicles might also be penalized by an RTG requiring a larger radiator than that of an equivalent thermionic system.

A modular space power generator composed of Isomite converters offers a highly redundant, integrated system of competitive efficiency and is superior to the RTG in specific power. Modular construction involving a relatively large number of separately fueled and completely independent power cells permits rapid development of generators "tailored" to an optimum size and configuration for specific mission requirements. The development costs of a family of generators covering a wide range of power would thus tend to be a modest increment to the investment required for development and qualification of a single module.

PHASE I PROGRAM OBJECTIVES

The objective of the Phase I effort is to establish parametric performance characteristics of three thermionic multicell generators with respective outputs of 50, 100, and 200 w_e. Output characteristics, efficiency, specific power, and weight are evaluated for practical ranges of dominant system variables. The influence of thermionic parameters, emitter geometry, fuel form, helium management, array reliability, system integration, and nuclear safety requirements are evaluated. The Phase I study program has five primary objectives:

1. To identify the influence of electrode surface parameters on the performance characteristics and growth potential of individual converters.
2. To define constraints imposed by choice of fuel form, emitter geometry, and helium management technique.
3. To optimize converter selection and interconnection based on requirements for generator reliability and voltage.
4. To evaluate off-design performance and characteristics of converters selected in Objective 3.
5. To determine the parametric weight and characteristics of a 50, 100, and 200 w_e generator based on the design inputs from Objectives 1 through 4.

PROGRAM APPROACH

The Phase I design study establishes the parametric performance and characteristics of three baseline generators in the power range 50 to 200 w_e composed of Isomite cell arrays in conventional aeroshell structures. Generator design and material selection reflect current or credible near-term technology (estimated availability within three years). A brief review of advanced concepts based on future (5 to 10 years) technology is included to illustrate the long-term growth potential of the concept.

A large number of variables are involved in a parametric study of a thermionic system. The scope of this design study has been limited by the assumption of these system conditions.

1. Generator design is not oriented to specific mission requirements.
2. Parametric studies relate to plutonia-fueled generators.
3. Generator characteristics are evaluated for terminal voltage from 3 to 10 v without electronic power conditioning.
4. Mission life of 10 years.
5. Converter performance analysis reflects the assumption of 1 mil electrode spacing and a zero-gravity operational mission environment.

Baseline Generator Configuration

The modular "building-block" of the multicell generator is the Isomite power cell shown typically* in Figure 1-1. The converter is powered by direct thermal conduction from a radionuclide fuel contained in the emitter capsule. A second capsule completely surrounds the thermionic emitter and functions as the collector substrate. Both electrode surfaces may be formed as treated surfaces of the substrate materials or by applied surface coatings. The electrode gap is maintained by spacing elements, which provide both thermal and electrical isolation of the emitter. A wire lead passes through an insulator in the collector and electrically connects the emitter to a terminal mounted on a ceramic/metal collector seal. A helium pressure relief tube could be substituted for the wire to form a combined emitter lead and venting device. The integral cesium reservoir is maintained at collector temperature and contained

*Detail differences from those shown in Figure 1 accommodate specific constraints of each application.

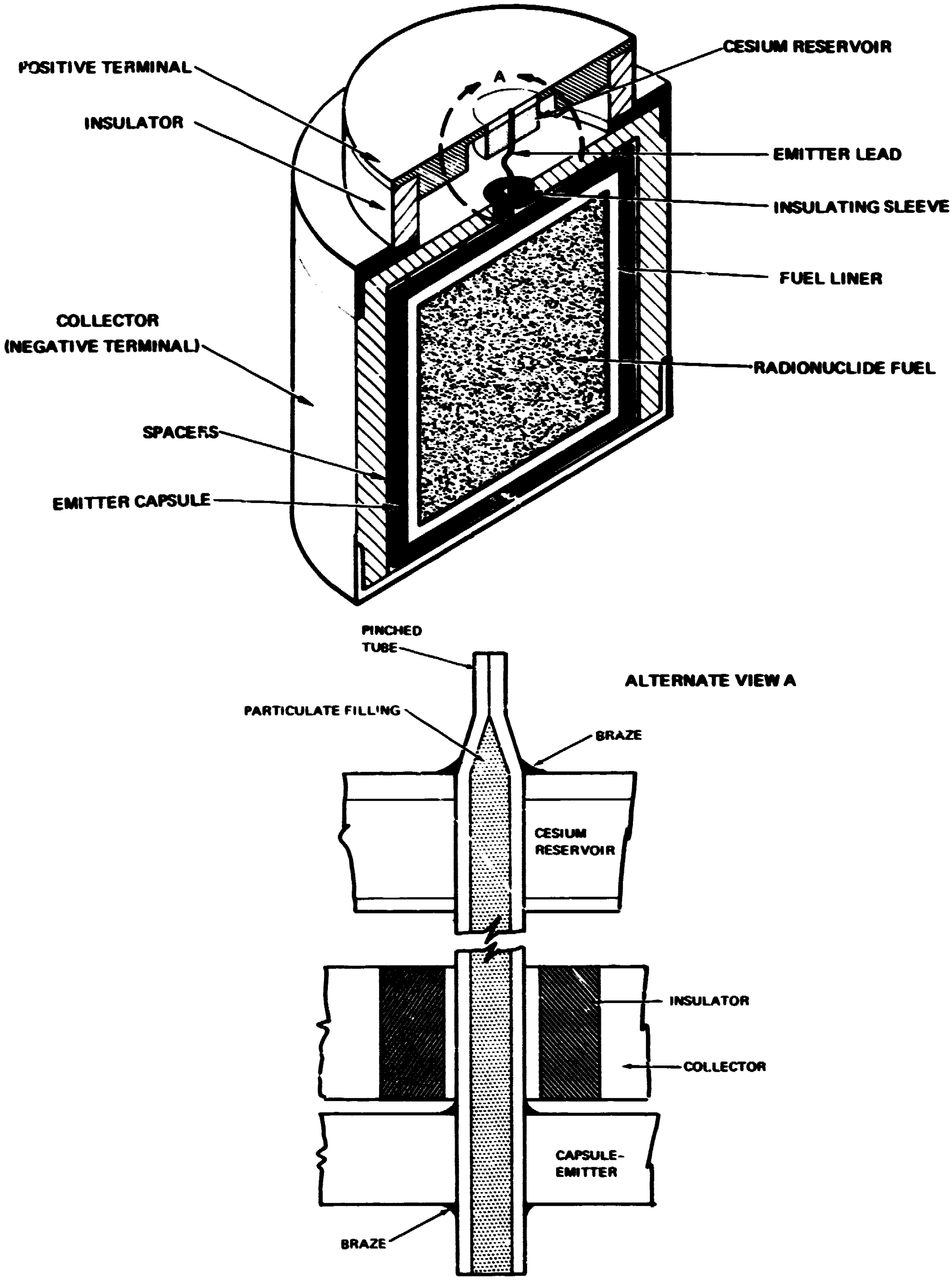

Figure 1-1. Isomite Power Cell

in the void region of the lead-through assembly. Low cesium vapor pressure (10^{-3} to 10^{-1} torr) establishes favorable emitter and collector work functions without contributing ion transport effects in the electrode gap.

The Isomite cell combines design features which are impractical under the operating conditions of conventional converters. In the Isomite design, structural components can be optimally designed to perform single or non-compromise functions. For example, the collector body forms a rugged secondary enclosure around the emitter and the lead can be sized separately to have an optimum aspect ratio. In contrast, the emitter lead in a conventional converter also forms part of the vacuum enclosure and its design therefore, is non-ideal in either function.

The basic configuration scales geometrically from 100 μw_e to several watts. Total enclosure of the emitter eliminates the relatively unscalable thermal leakage contributed by lead conduction and radiation, which limits the minimum size of an efficient conventional converter module to approximately 20 w_e. Thermal flux concentration to match the fuel thermal power and thermionic surface flux density is not a fundamental requirement in the vacuum mode converter. Optimum cells can be designed to accommodate all practical fuel power densities above approximately 1 w_t/cm^3.

Generator Aeroshell and Reentry Vehicle System

The Isomite cells which comprise the generator are considered to be arranged within a structure which provides an operational housing during mission life, launch pad abort debris protection, and intact reentry disposal. Reentry vehicle concepts which could be applied include the blunt cone (used in Isotope/Brayton power systems), flared-cylinders, high-drag cubes, rectangular parallelepipeds, and flat plates (References 4, 5, and 6). For the parametric Phase I design study, the flared-cylinder concept is selected as a characteristically low-weight (not necessarily minimum weight) housing/reentry vehicle system which is scalable to accommodate Isomite cell arrangement patterns. This concept is also considered to require a minimum of development to provide an acceptable level of safety. The flared-cylinder has undergone development in ICBM programs as the shape of Mark 3 and Mark 4 warheads.

The flared-cylinder concept is illustrated in Figure 1-2. A multicell converter array, series/parallel connected for maximum electrical reliability, is arranged within an ellipsoidal-ended cylinder with a ribbed impact plate and crush-up in the nose section. To protect the generator against reentry heating, a POCO graphite ablator covers the whole aeroshell exterior except in the region of the mounting ring. A metal shell provides a chamber for vented helium and additional structural protection against debris and over pressure in launch pad explosions. The flared cone supplies aerodynamic drag to limit terminal impact velocities and earth burial. The aspect ratio and weight distribution of the aeroshell is designed to ensure that the center of pressure is on the axis of symmetry between the center of mass and the cone. This ensures proper orientation of the aeroshell during reentry.

Parametric Design Approach

The characterization of multicell generators is established by the parametric design approach shown in Figure 1-3. Two major subsystems, the

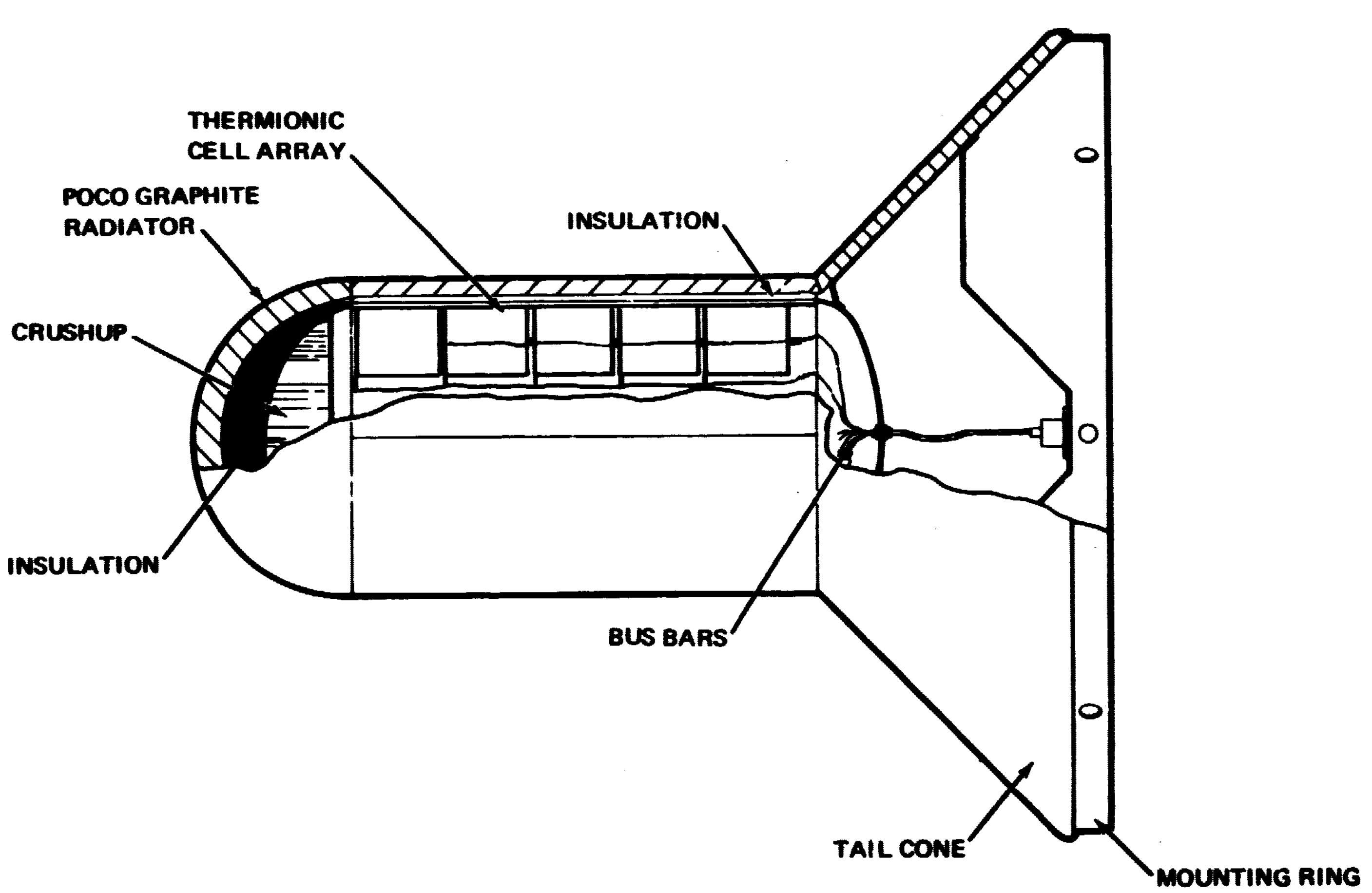

Figure 1-2. Multicell Generator Configuration

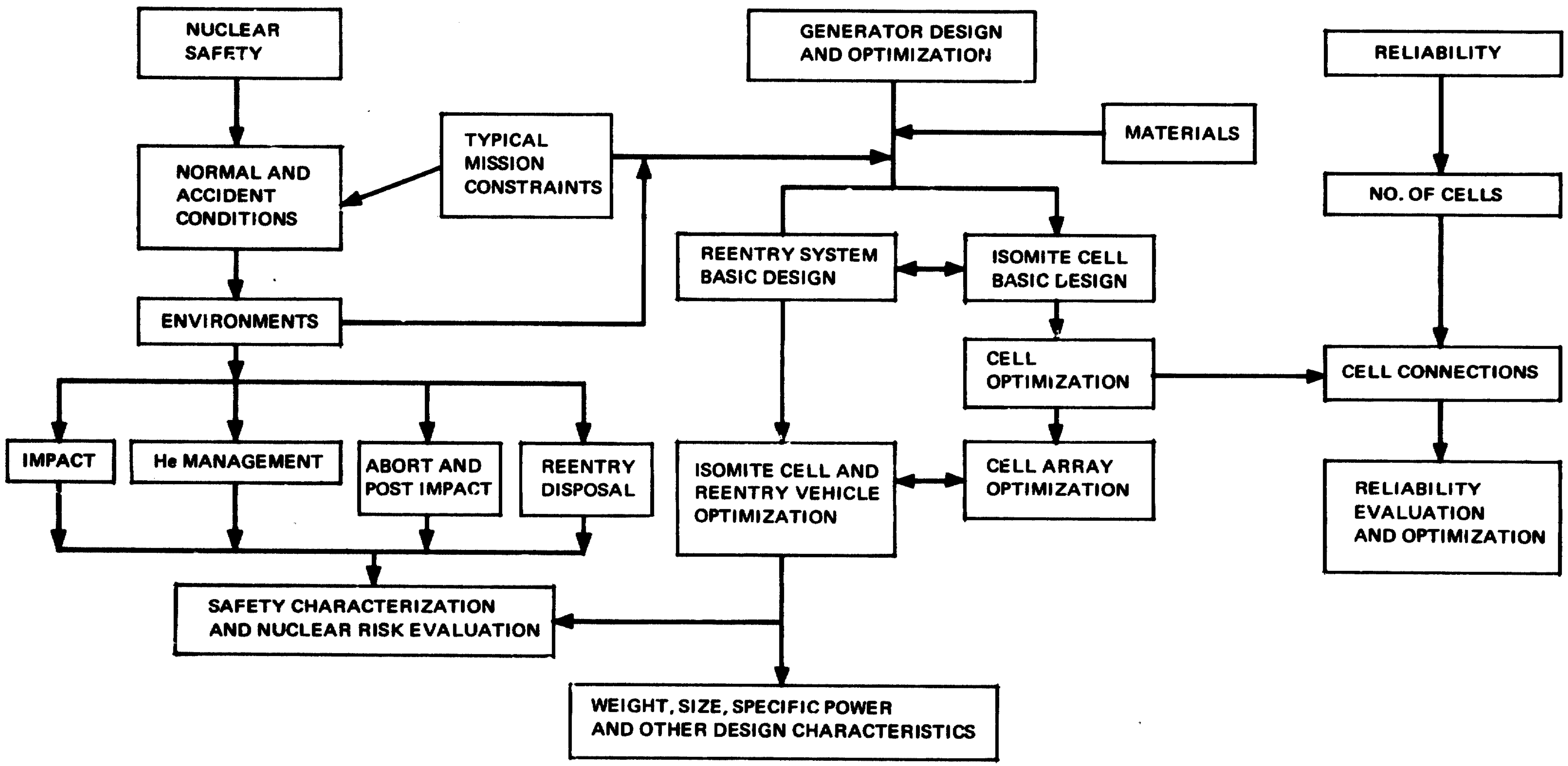

Figure 1-3. Flow-Diagram for Parametric Design Approach

converter array and aeroshell, and their interactions, are identified. Generator design and optimization requires consideration of basic converter design and performance optimization iteratively constrained by mission and aeroshell characteristics. Converter performance is established by choice of fuel, electrode materials, emitter geometry, and helium management techniques. Selection of the multicell array is constrained by the available range of converter module power, credible current-technology components, and system design goals for reliability and generator voltage.

Aeroshell design involves identification of nuclear safety requirements for normal mission operation and accident conditions. Typical mission constraints and environments govern materials selection and design of structure to survive abort, reentry disposable, impact, and post-impact conditions. The design of the aeroshell also reflects the requirement to match thermal characteristics of the converter array.

System integration of the generator is provided by electrical connections and components which isolate the aeroshell from mechanical shock and vibration transmitted from the space vehicle. The system-integrated generator is characterized by its weight, size, specific power, reliability, and output voltage. Characteristics of the converter array, aeroshell, and minimum-penalty system-integration components are considered. The aeroshell design establishes the safety characterization of the system and the extent of nuclear risk during its deployment.

The balance of this report is arranged as follows.

- Section 2 Influence of electrode surface parameters.
- Section 3 Constraints imposed by choice of fuel form, emitter geometry, and helium management technique.
- Section 4 Converter selection and interconnection based on generator reliability and voltage.
- Section 5 Off-design converter performance and characteristics.
- Section 6 Aeroshell optimization.
- Section 7 Generator characterization and advanced-technology review.
- Section 8 Conclusions and recommendations.

Section 2
ELECTRODE SURFACE PARAMETER INFLUENCE

The Isomite cell behaves thermionically as a space-charge limited converter with a potential energy diagram as shown in Figure 2-1. Potential distribution in the electrode gap has been described in detail (References 7 and 8). With electrode spacing on the order of 1 mil, the converter operates with useful efficiencies at emitter temperatures below 1400°K if ϕ_e and ϕ_c are less than approximately 2.4 and 1.8 ev, respectively. Surface work functions of this magnitude are obtained by partial monolayer adsorption of cesium on refractory metal surfaces operating in the conventional collector regime of the Rasor-Warner ϕ vs T/T_R diagram (Reference 9). In the Isomite converter, cesium vapor pressures from 10^{-3} to 10^{-1} torr produce favorable work

70-894

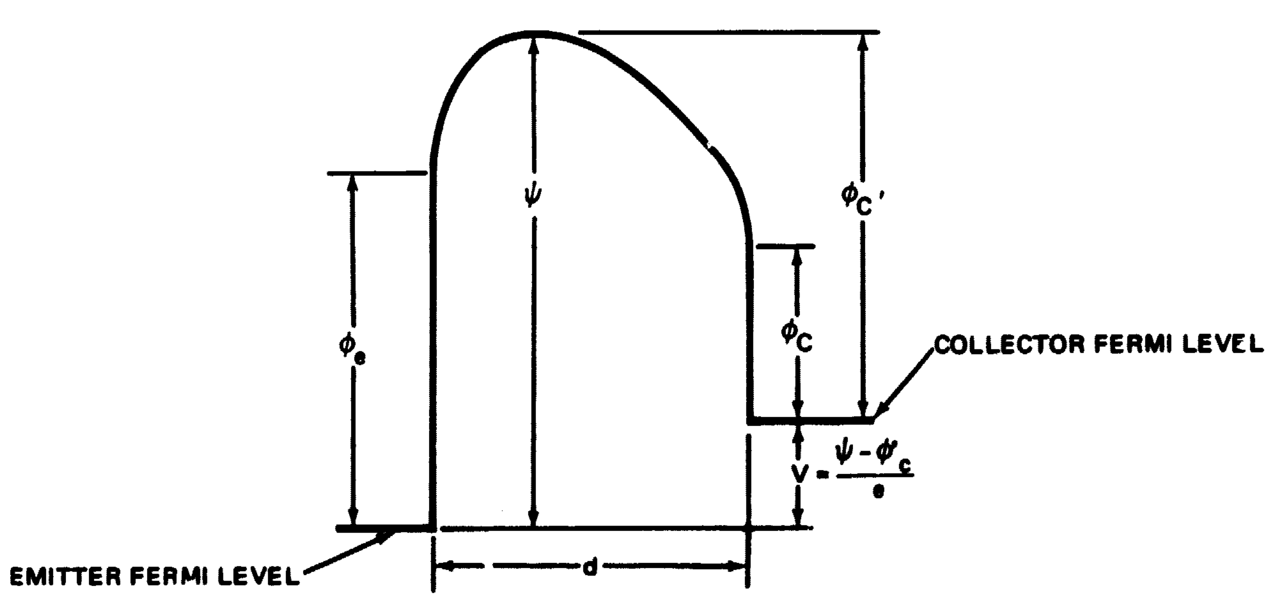

Figure 2-1. Space-Charge Limited, Vacuum-Mode Converter Potential Diagram

functions on the electrode surfaces without contributing ion transport effects in the converter.

Converter efficiency is defined by the ratio of useful power at the converter terminals to the sum of the components of the thermal energy balance. Figure 2-2 shows the apportionment of thermal losses for a typical converter. The dominance of Q_r and Q_e indicates the value in selecting electrode surfaces with low emissivities and low ϕ_{min} occurring at relatively high T/T_R values to minimize cesium vapor conduction.

ELECTRODE SURFACES

Three electrode surface systems are currently under investigation at DWDL:

1. DWDL-developed Ta-O-Cs emitter and collector.
2. W-Cs emitter and Ta-O-Cs collector.
3. Langmuir W-O-Cs emitter and collector.

70-895

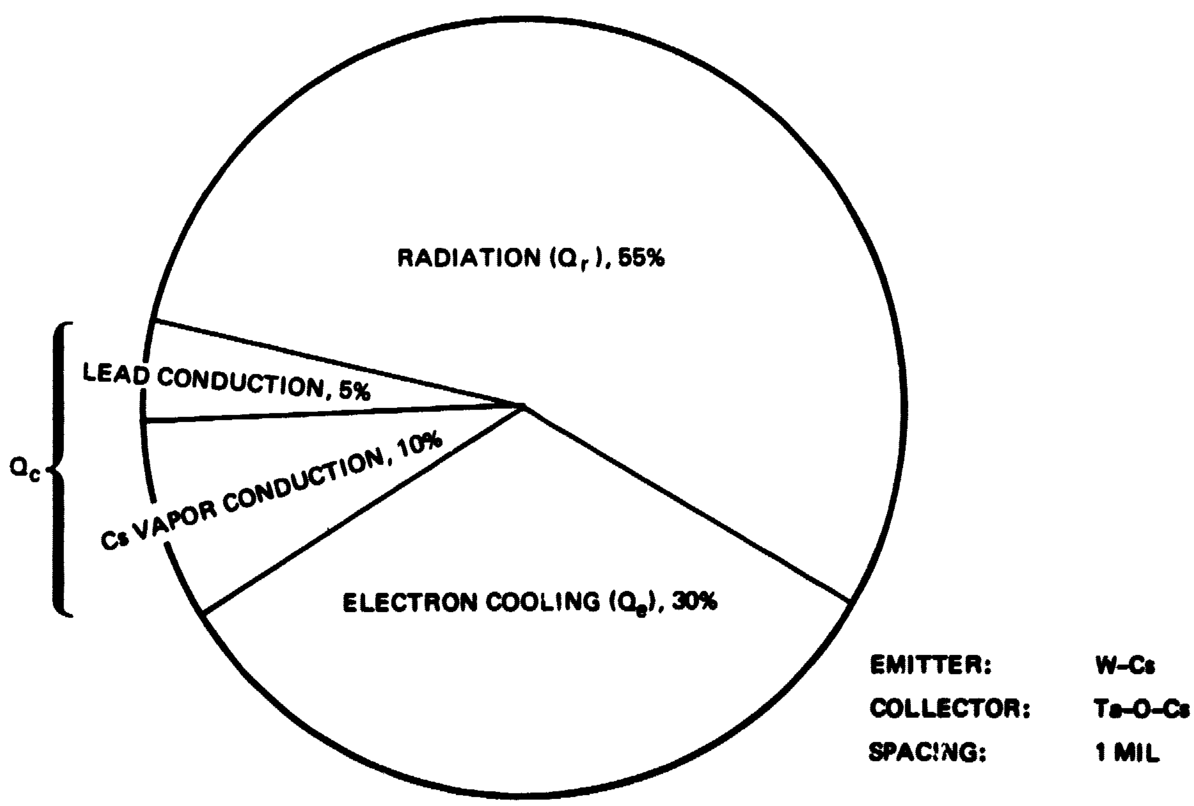

Figure 2-2. Apportionment of Thermal Losses For an Optimized 5 We Space Power Converter

Ta-O-Cs surface systems have been reduced to practice, used in over 50 radionuclide-fueled and electrically-heated converters, and have accumulated nearly 100,000 hours operation. Surfaces can be prepared reproducibly to achieve ϕ_{min} between 1.34 and 1.64 ev over the range of collector temperatures usually required in the Isomite converter. The Ta-O-Cs surface also provides acceptable values of ϕ_e (1.7 to 2.3 ev) over a range of T_e from 900° to 1400°K.

Characteristics of the Ta-O-Cs surface svstem are not totally understood in the ϕ_{min} region. Laboratorv experience with the DWDL-proprietary surface shows a general temperature dependence of ϕ_{min}; however, the exact nature of this dependence is still under investigation in Independent Research and Development (IRAD) programs. For the computational purposes of this study, recent laboratory data have been correlated by straightline approximations to describe the temperature dependence of ϕ_{min} to first order accuracy (Figure 2-3). Data which permit this refinement have been generated concurrently with the progress of this design study and therefore, converter performance summarized in this report supersedes characteristics in previous monthly summaries which did not take this temperature dependence into account.

The W-Cs emitter is of interest because of its relatively lower emissivity than that of the Ta surface (References 10 and 11). The W-Cs surface (Reference 12) ϕ vs T/T_R characteristic is not significantly higher than that of the Ta-O-Cs surface in the emitter region. The surface combination W-Cs emitter and Ta-O-Cs collector offers a lower Q_r loss component in some regions of the optimized converter power range.

The Langmuir W-O-Cs system (Reference 13), when plotted on the ϕ vs T/T_R plane (Figure 2-4) has rather remarkable characteristics, and three significant potential advantages compared with the two electrode systems considered so far.

1. Electrode emissivity can be expected to approach that of clean tungsten.
2. Values of ϕ_{min} and its temperature dependence are comparable with those of the Ta-O-Cs surface.
3. The ϕ vs T/T_R characteristics show ϕ_{min} at significantly higher values of T/T_R.

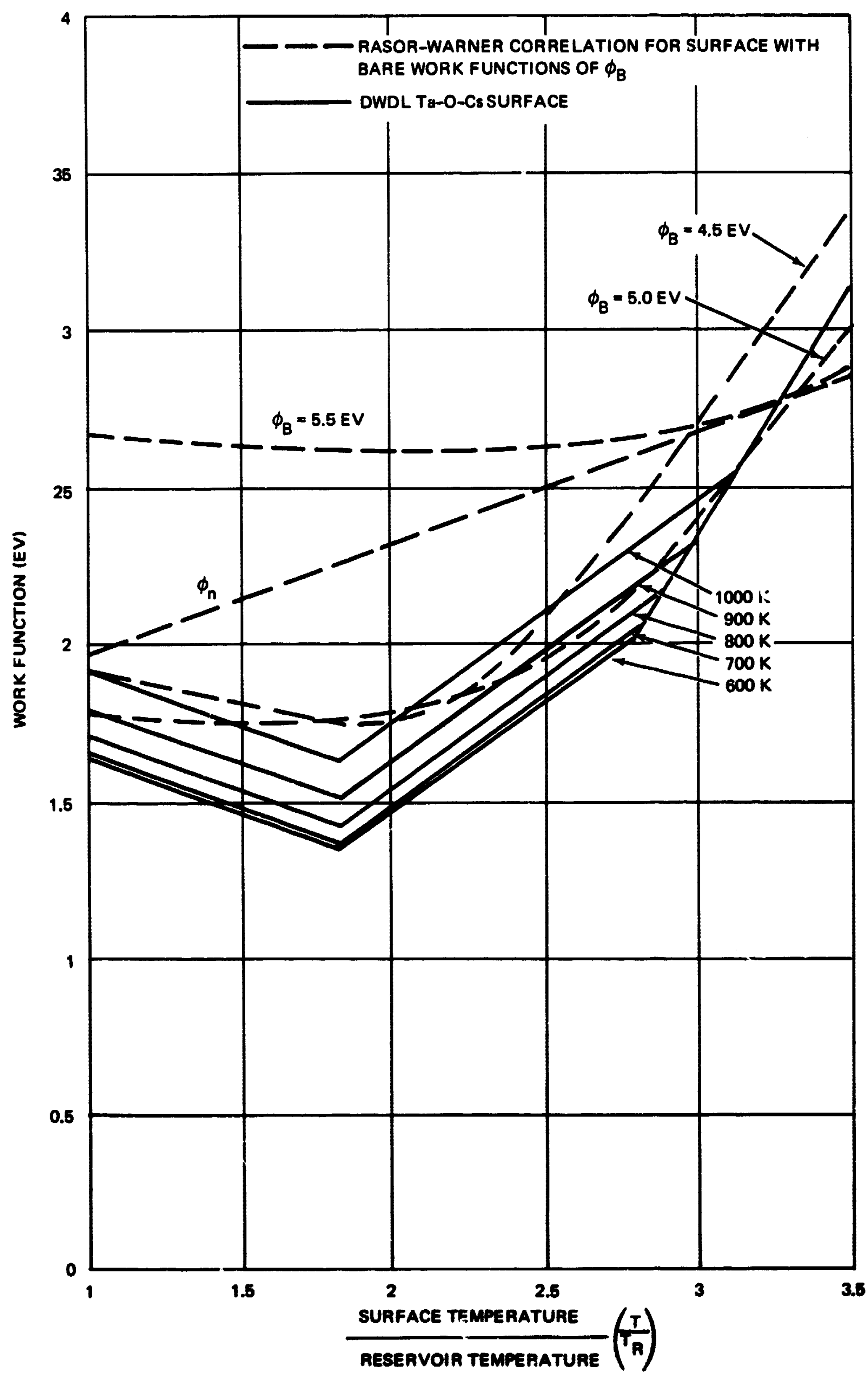

Figure 2-3. Work Function vs T/T_R Characteristics for the Ta-O-Cs Surface

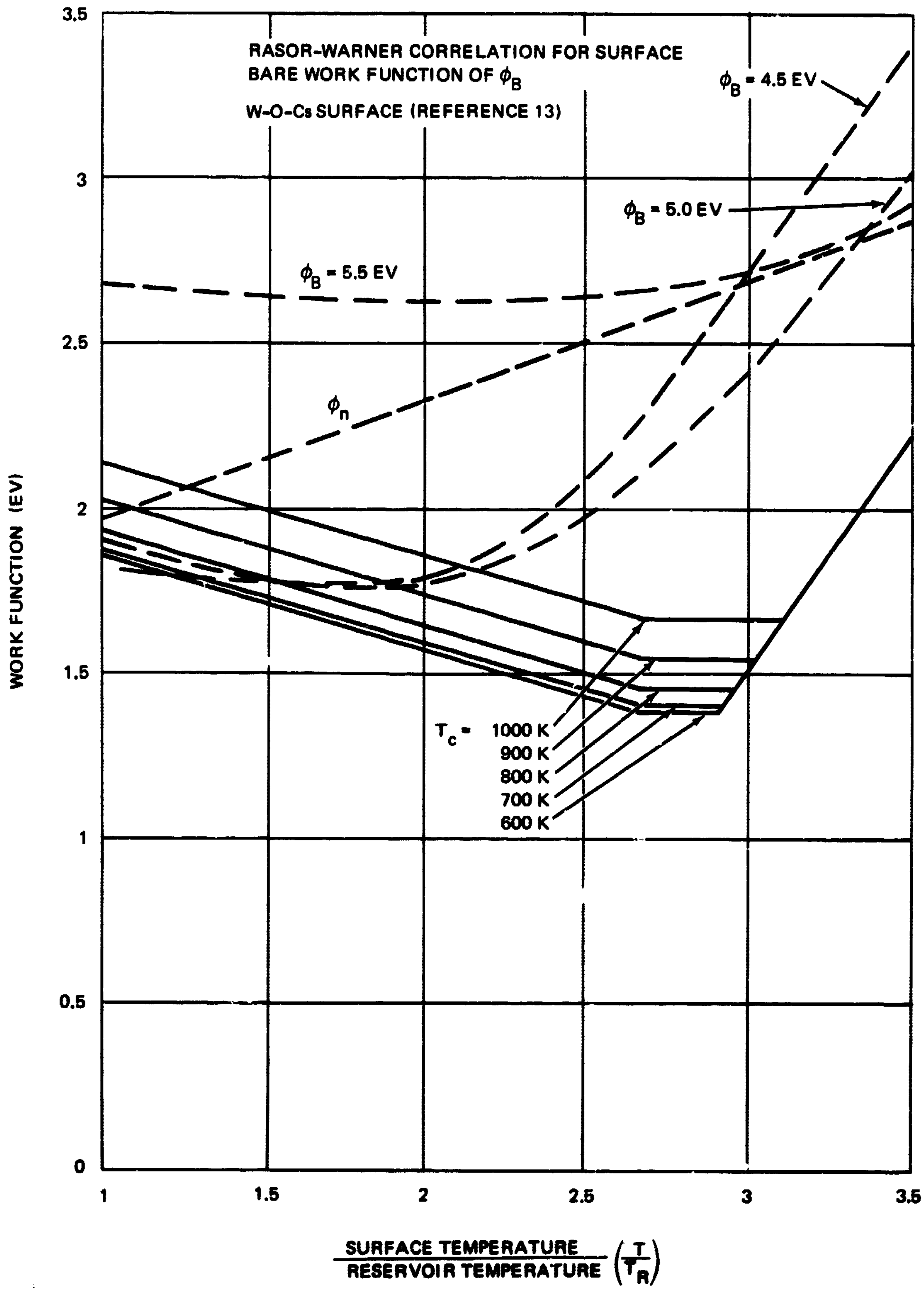

Figure 2-4. Work Function vs T/T_R Characteristics for the W-O-Cs Surface

The W-O-Cs surface offers an operational domain in the ϕ vs T/T_R plane far removed from the Rasor-Warner envelope for conventional refractory metals. A potential disadvantage (compared with the Ta-O-Cs system) may be that W-O-Cs surfaces depend apparently on the maintenance of an atomic oxygen monolayer, whereas oxygen in the Ta-O-Cs system appears to be contained in bulk solid solution. Corrosion of the Ta-O-Cs electrode surface may, therefore, tend to be repaired by a dispensation process from the substrate, in contrast to the tungsten-based surface, which may suffer irreparable degradation if the surface-active oxygen were removed by impurity reactions during the converter life.

COMPUTATIONAL APPROACH

The performance of optimized vacuum-mode converters is reviewed in the range of Q and A from 10 to 100 w_t and 10 to 100 cm^2, respectively. With the surface systems under review, cell module power between 1 and 10 w_e is achieved for this range of Q and A. DWDL experience shows this range of converter power to be the general range of interest for a multicell generator design between 50 and 200 w_e. A DWDL-developed computer code is used to calculate cell characteristics and describe converter performance parameters as functions of Q/A. In these calculations, all cell thermal loss mechanisms applicable to a general space mission environment are considered. The Q/A dependence of performance parameters results from all components of the energy balance, with the exception of support conduction loss, being emitter area dependent. Laboratory measurement of emitter support loss (typically in the range 1 to 3 $mw_t/°K$ on earth) shows that it becomes negligible for the very small gravitational loads typical of most space missions. When support loading occurs (for instance, in spin-stabilized vehicles or planetary lander missions) it can be accounted for by adding an additional component to the input thermal inventory. A parametric comparison of cell characteristics, ignoring the non-area-dependent thermal loss, is considered adequate for the Phase I study. Specific mission-imposed constraints can be considered as refinements in the Phase II design effort.

Figure 2-5 shows the logic of the DWDL-developed multiple iterative computer code used to determine optimum vacuum mode converter parameters for a given Q and A. Initial assumptions are made for ℓ/a, ψ, and T_C.

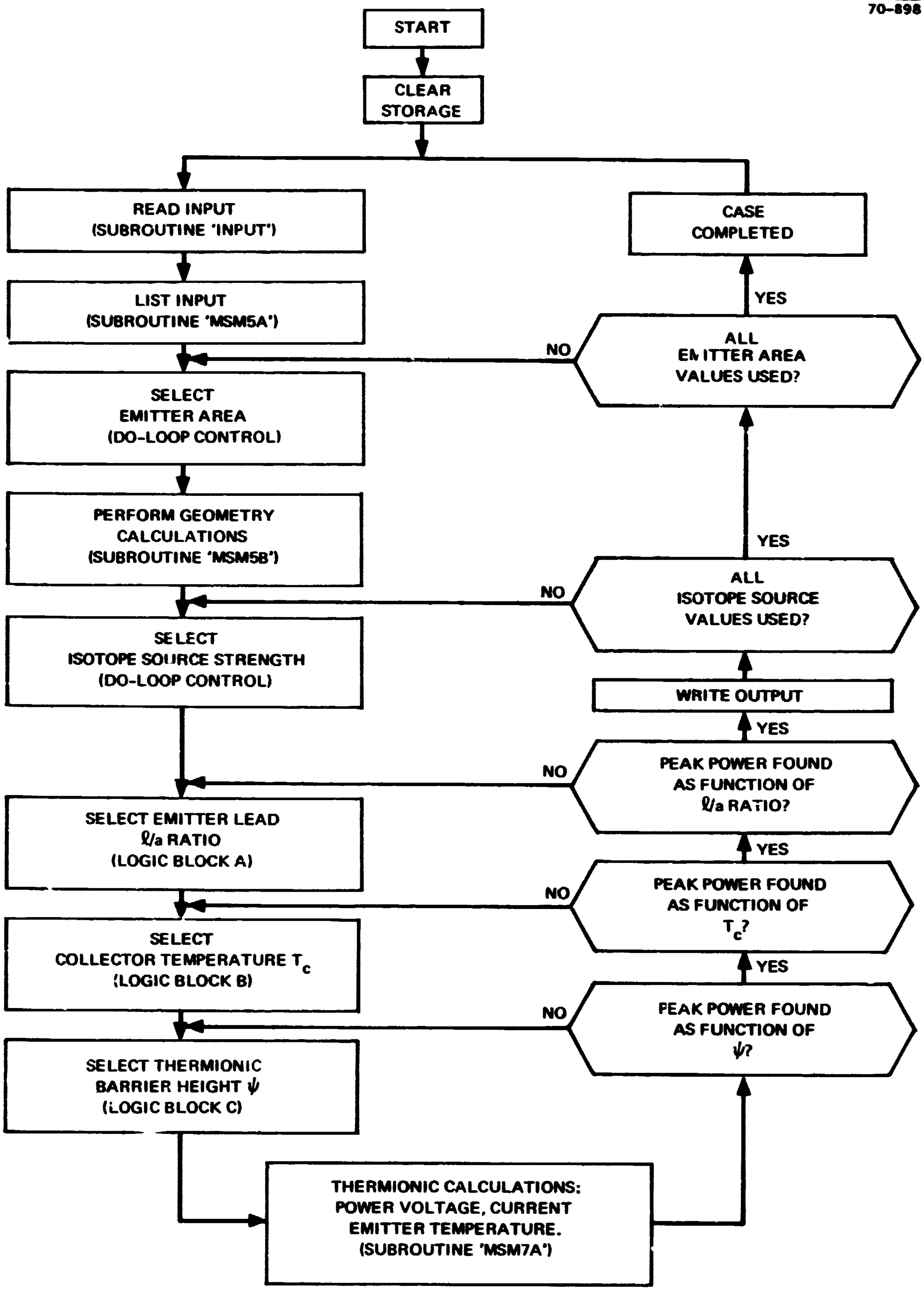

Figure 2-5. Logic Flow Diagram of DWDL Vacuum-Mode Converter Computer Code

With these parameters, a heat balance is obtained for the emitter by varying T_e. The heat bal. ce is calculated using temperature-dependent expressions for ϵ, ϕ_e, ϕ_c, and ℓ/a. The remaining converter characteristics are then uniquely determined by Q, A, ℓ/a, ψ, T_c, and T_e. A second estimate is made for ψ, the process is repeated, and iteration proceeds on ψ until the peak power obtainable for a given Q, A, ℓ/a, and T_c is calculated. A new estimate is then made for T_c, followed by a complete sequence of iterations on ψ (ψ-loop). Iteration on T_c continues (T_c-loop) until the peak power is found for specified values of Q, A, and ℓ/a. The outer loop consists of a search for the ℓ/a which results in the highest electrical output power. A complete calculation, taking approximately 6 to 10 minutes on the IBM 1130, requires about 7 values of ℓ/a, each with about 10 T_c-loops, iterating 10 ψ-loops per T_c-loop. In total, approximately 700 thermionic calculations are required for each Q/A combination. Detailed operational and functional relationships of this code will be presented in the final report.

Converter optimization is obtained in this manner, independent of emitter geometry. All characteristics, however, are strongly influenced by electrode spacing, which has been chosen, for the purposes of this study, at 1 mil. This spacing represents developing technology in laboratory devices and is consistent with the credibility of building converters with thin-wall emitter and collector capsules several centimeters in diameter. The effect of off-design variation in electrode spacing is considered in Section 5.

PERFORMANCE COMPARISON

Parametric comparisons of optimum vacuum-mode converter characteristics are presented in Figure 2-6 through 2-9 showing the influence of three electrode surface combinations. Two of the three combinations are worthy of consideration later in this study. The W-Cs emitter/Ta-O-Cs collector combination is only marginally more efficient (Figure 2-6) than the totally Ta-based surface system in the Q/A <1 range. It will become evident in Section 3 that fuel, geometry, and helium management choices can be arranged to exploit converter performance at higher values of Q/A, where Ta-O-Cs is the superior current technology electrode choice. Further consideration of the W-Cs emitter/Ta-O-Cs collector combination is not warranted in the Phase I study.

The W-O-Cs surface system has not yet been reduced to practice in a laboratory converter. The surface system provides, however, potentially superior conversion efficiency and higher cell output voltage (Figure 2-7). Potential disadvantages evident in Figure 2-8 are higher emitter and lower collector temperatures which might tend to prejudice materials compatibility and compact generator radiator sizing, respectively. The potential advantages appear to outweigh disadvantages and therefore the W-O-Cs surface will be considered in the summary of advanced technology growth potential.

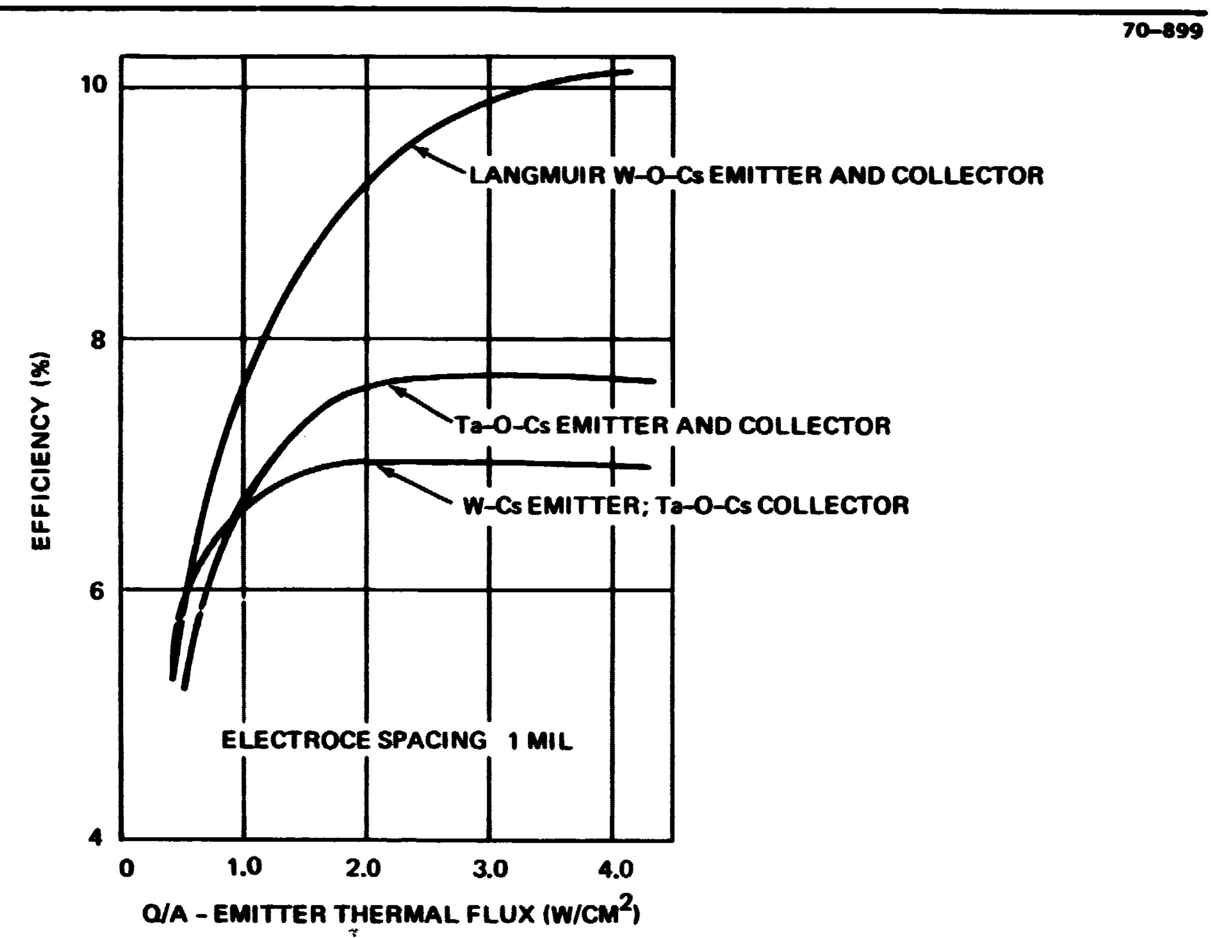

Figure 2-6. Efficiency vs Emitter Thermal Flux at Optimum T_c/T_R

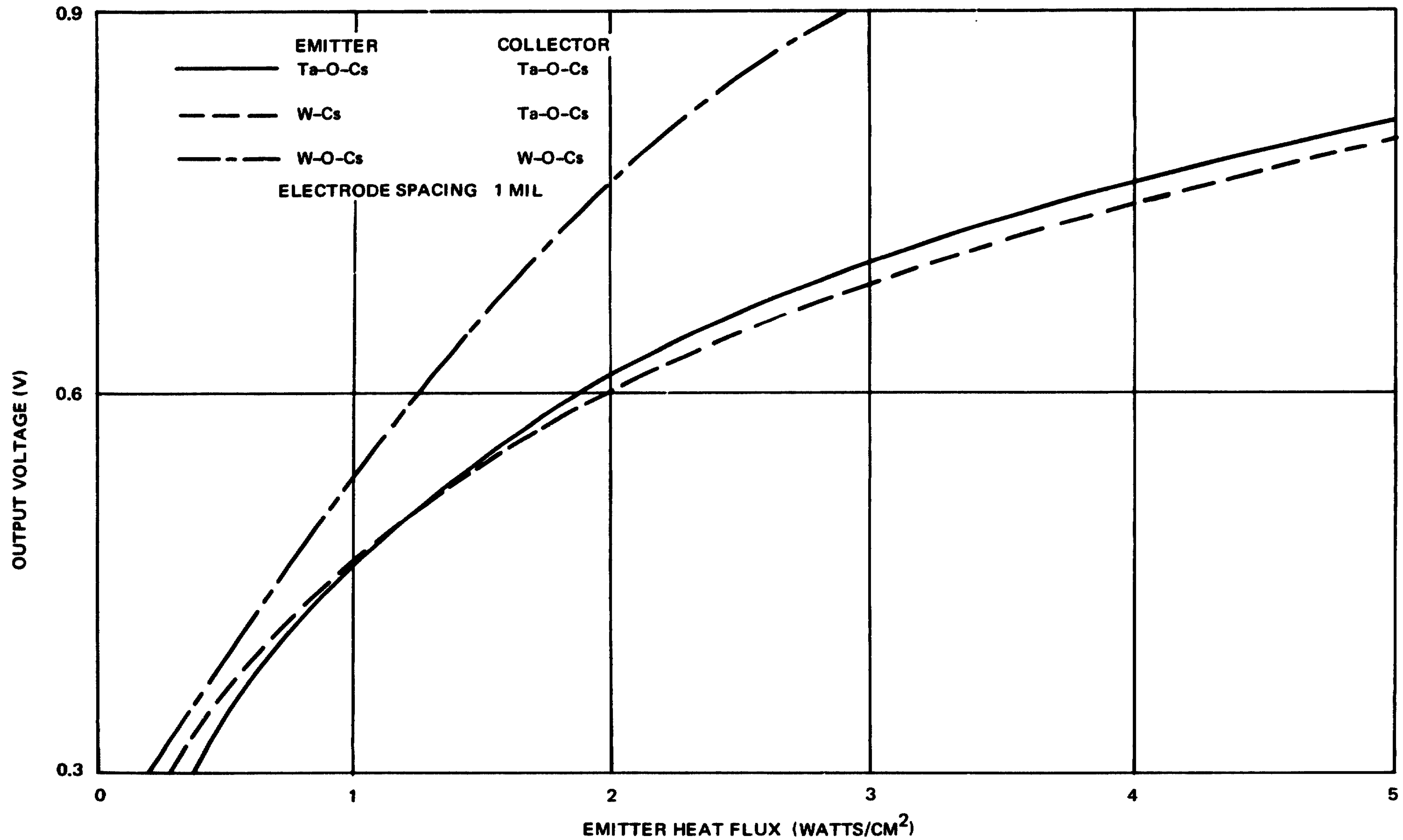

Figure 2-7. Output Voltage vs Emitter Thermal Flux at Optimum T_c/T_R

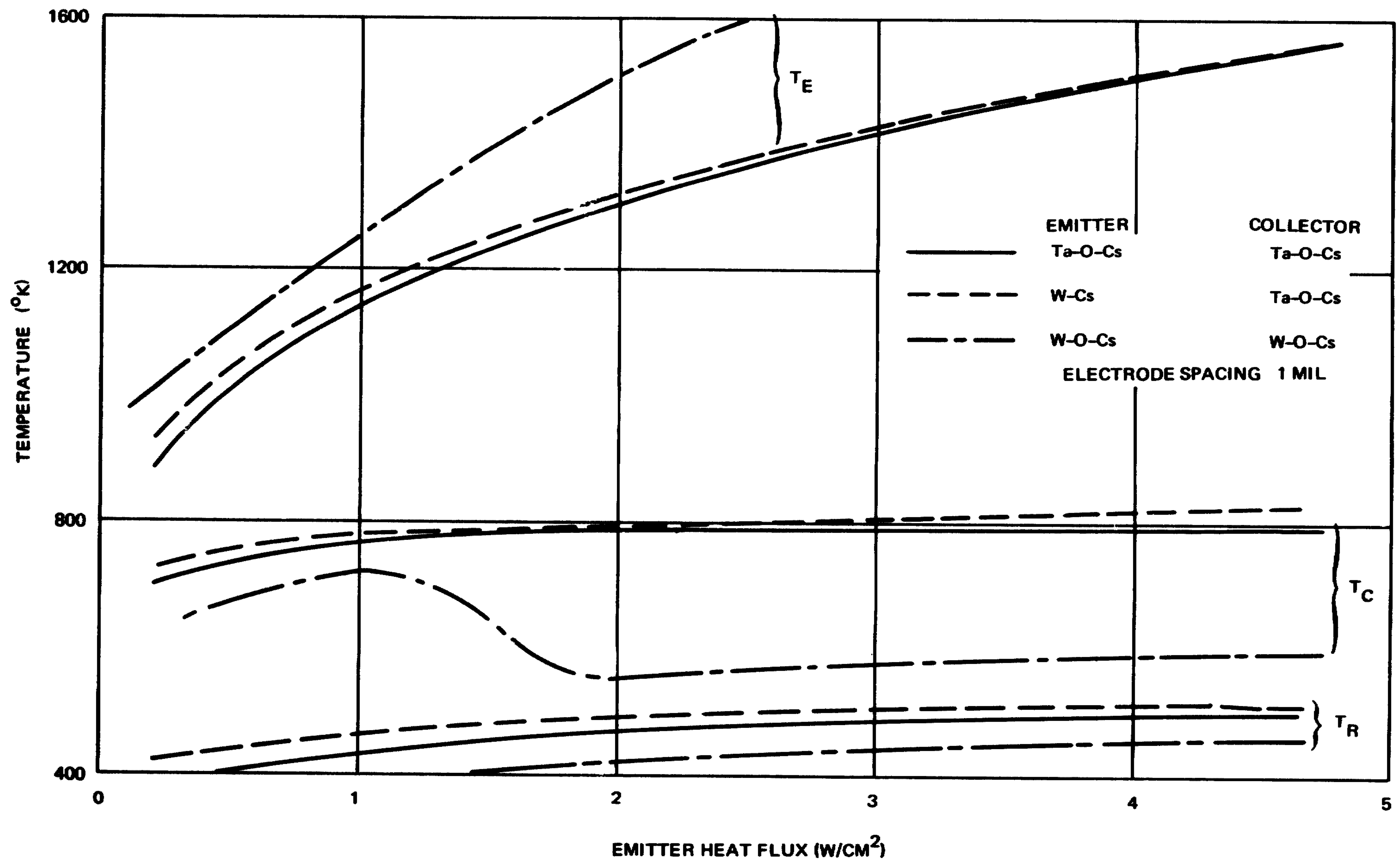

Figure 2-8. T_E, T_c, and T_R vs Emitter Thermal Flux

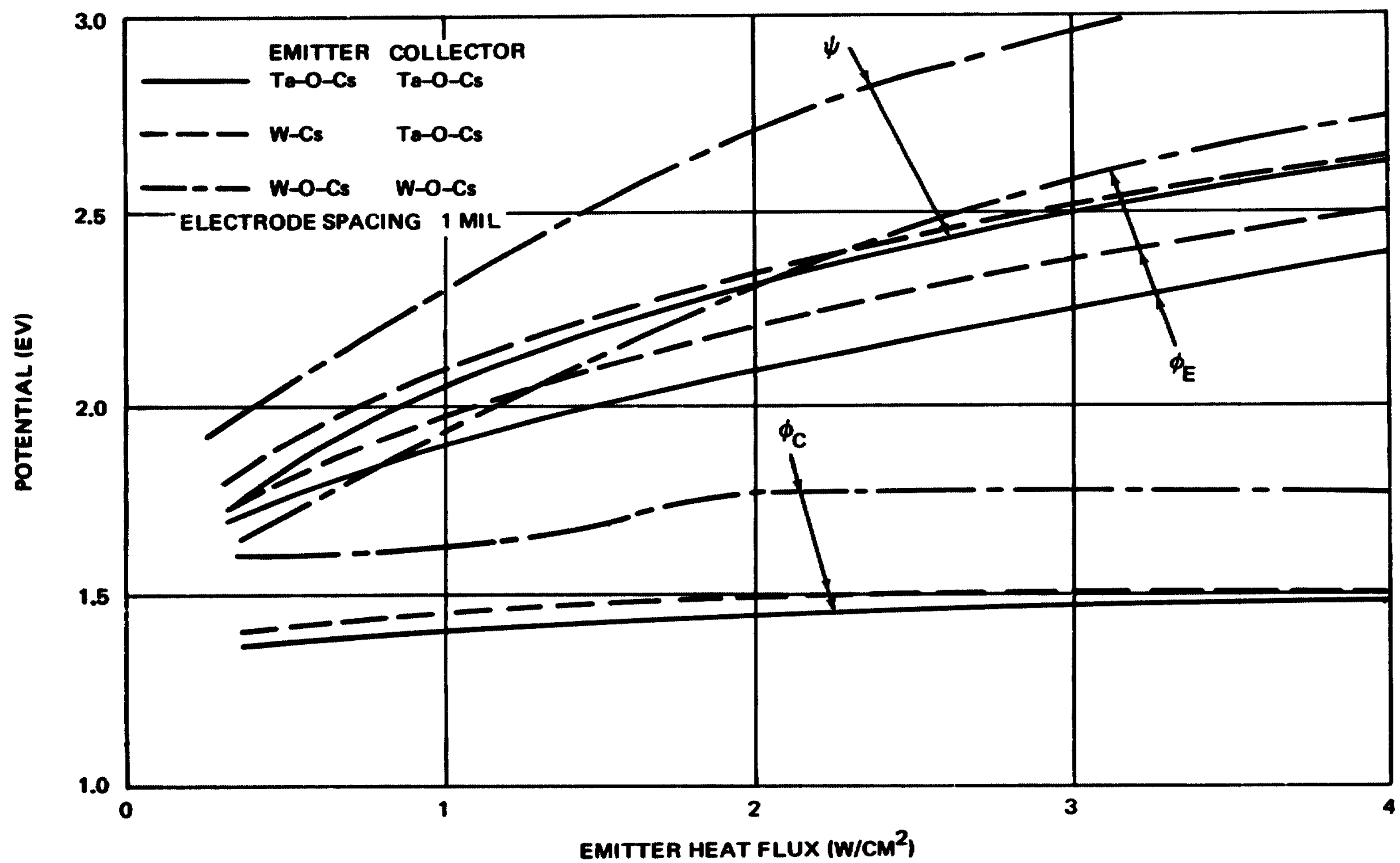

Figure 2-9. ψ, ϕ, and ϕ_c vs Emitter Thermal Flux

Section 3
FUEL, EMITTER GEOMETRY, AND HELIUM MANAGEMENT CONSTRAINTS

The choice of radionuclide fuel, emitter geometry, and helium management techniques determines what fraction of the Q/A range is available in a practical converter design. It was established in Section 2 that most converter performance parameters increase monotonically with Q/A. Constraints which permit high Q/A design are, therefore, to be desired.

FUEL CONSTRAINTS

For a given emitter capsule geometry and helium management choice (vented or unvented capsule), a fuel thermal inventory limit is established by the fuel form and its effective thermal power density. Figure 3-1 shows fuel load limits on a logarithmic Q vs A plane for three radionuclide fuels in vented spherical capsules with a 25-mil wall thickness. Isopower curves (P_{max}) are plotted in Figure 3-1 for optimum converters with Ta-O-Cs surfaces and 1-mil electrode spacing.

The fuel forms considered are:

1. Plutonia Solid Solution Cermet (SSC)
2. Plutonia Cermet
3. Curia Cermet

Table 3-1 summarizes plutonia fuel form properties (Reference 14 and 15)

The curia fuel curve shown in Figure 3-1 is the prediction (Reference 16) of a potentially feasible curia cermet with a density of 10.5 g/cm^3 and a power density of 19.1 w_t/cm^3. Consideration of this fuel relates to the future technology review in Section 7.

Figure 3-1 shows that, by increasing the effective thermal power density, the fuel load limit curve allows converter design at progressively higher and generally more favorable Q/A values. The region to the left of each load limit

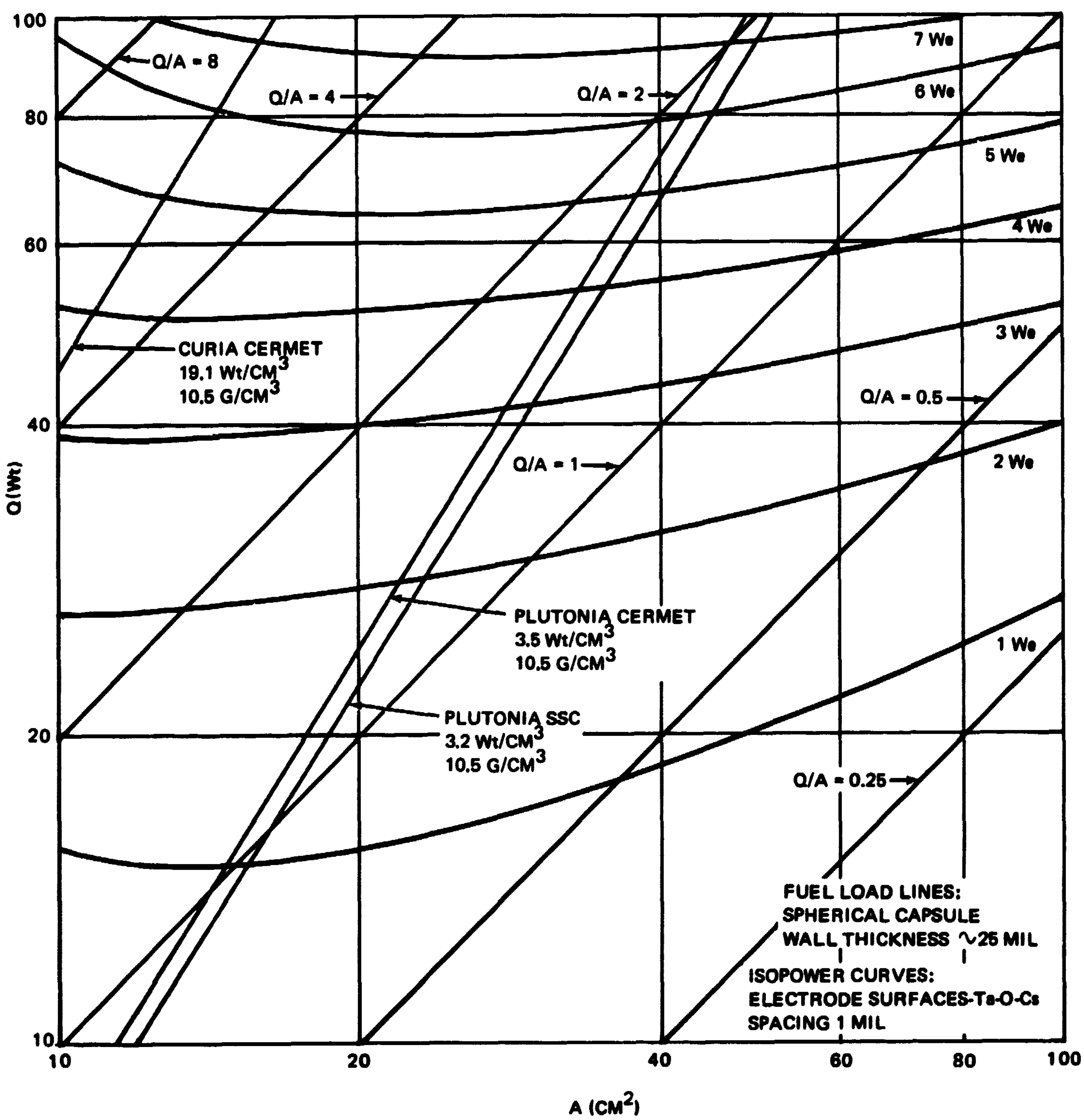

Figure 3-1. Fuel Load Limit for Three Fuel Forms on Q vs A Plane

Table 3-1

PLUTONIA FUEL FORM COMPARISON

Property	Plutonia Solid Solution Cermet	Plutonia Cermet
Density (g/cm^3)	10.5	10.7
Power Density (w_t/cm^3)	3.2	3.5
Thermal Conductivity (w_t/cm-°C):		
900°C	0.102	0.148
1200°C	0.098	0.146
Thermal Expansion (%ΔL/L) (20° to 900°C)	0.53	0.85

curve is unavailable for converter design in devices with all surfaces active. Operation to the left of the load limit line can be achieved by operating a fraction of the emitter thermionically and shielding other portions with insulating material. A similar plot is obtained with isopower curves for any other surface system by plotting P_{max} vs Q/A (derived from Figure 2-6) on the Q vs A plane.

The loci of best converter designs are intersection points of the fuel load and P_{max} curves in Figure 3-1. The fuel constraint imposed on converter specific power is compared in Figure 3-2 for several fuel and electrode surface combinations. Specific power rises with converter power and tends toward a plateau above 3-w_e module sizes. Increasing fuel thermal power density and improved electrode technology allow higher specific converter power. The plutonia cermet provides only a slight increase in specific power compared with that of the plutonia SSC for a given surface system. Interest in the plutonia cermet is now academic with regard to system applications because of the AEC's decision in midyear 1969 to concentrate on the plutonia SSC fuel form. Further reference to plutonia cermet is therefore not considered in the Phase I study.

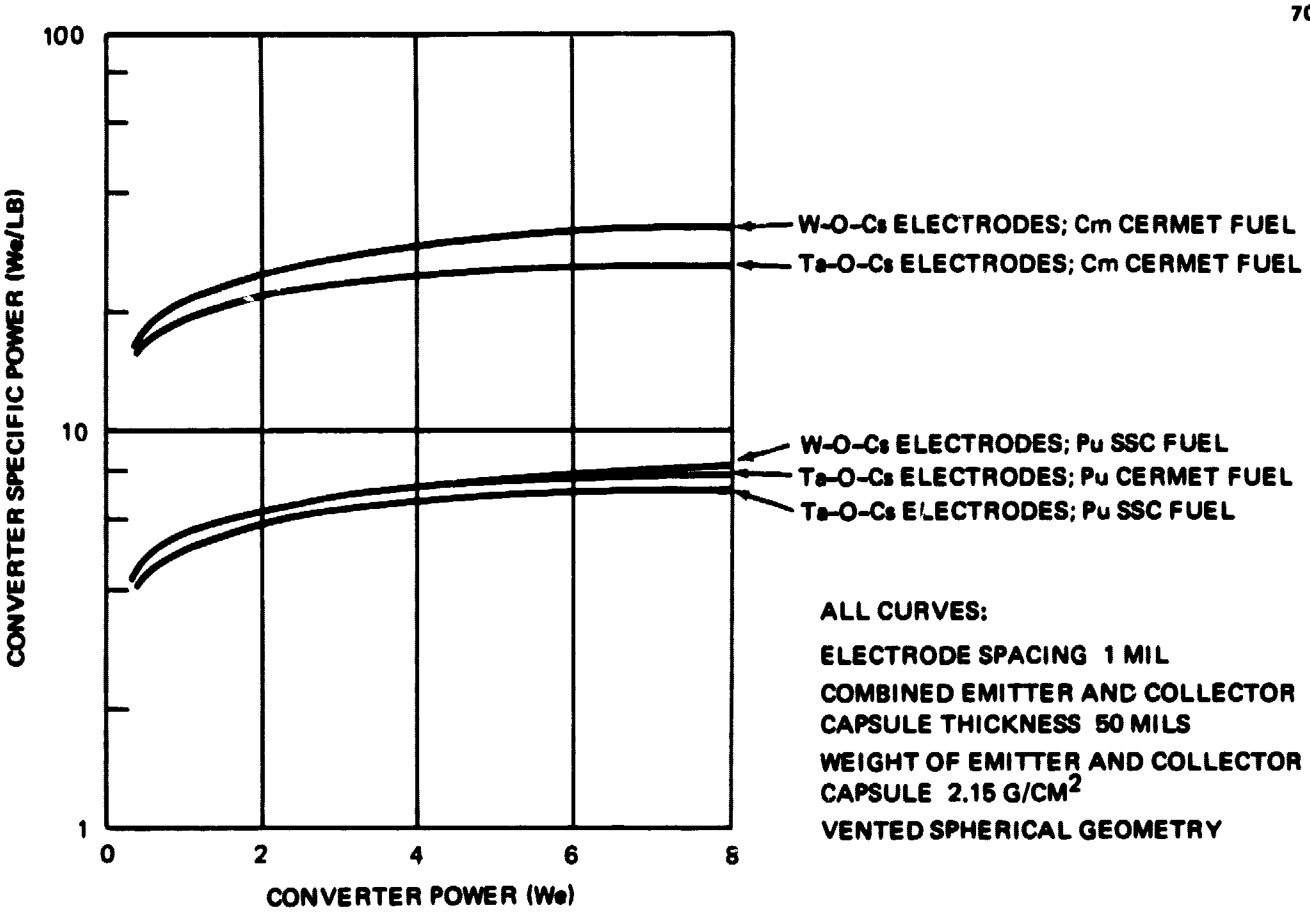

Figure 3-2. Converter Specific Power vs Cell Power Showing Fuel Load Constraint for Spherical Geometry

EMITTER GEOMETRY CONSTRAINT

Emitter geometry has an influence on converter design analogous to that of the fuel load limit. For a given fuel choice, helium management technique, and capsule wall thickness, the emitter geometry constraint (again fuel load limit) is a curve on the Q vs A plane (Figure 3-3). The Q/A region to the left of the geometry effect curve is excluded from use in a practical converter except, as previously noted, when the emitter is partitioned into thermionically active and inactive areas.

For converters with all of the emitter surface thermionically active, the progression from spheres to cylinders with increasing aspect ratios moves the design cut-off towards the right of the Q vs A plane and hence to lower Q/A and to a less favorable thermionic operational regime.

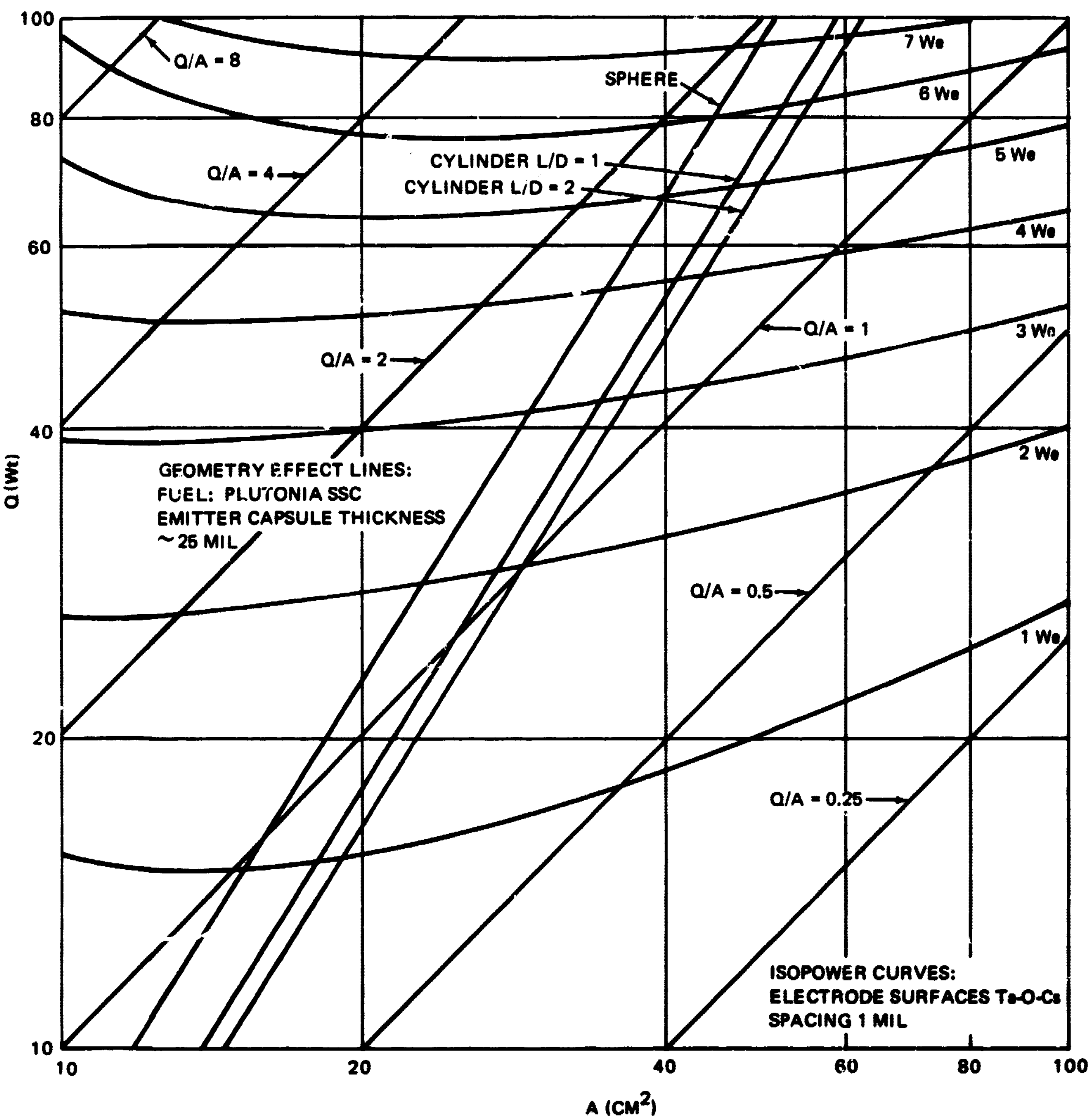

Figure 3-3. Geometry Effect Fuel Load Limit for Three Emitter Shapes on Q vs A Plane

HELIUM MANAGEMENT CONSIDERATION

Figure 3-4 shows the fuel load limits imposed by vented and unvented capsules of spherical and cylindrical form, respectively. The vented capsule curves are those of Figure 3-3. The unvented spherical capsule curve represents the load limit of the lightest weight T-111 capsule required to contain plutonia SSC fuel for a mission life of 10 years and survive temperature exposures 100°K above T_{eo} at mission EOL. The strength of a 25-mil thick collector capsule was taken into account to establish the most favorable unvented capsule design of comparable specific power to that of vented devices; the emitter would yield to take up the electrode spacing distance and then be reinforced by the collector. Calculation of the unvented cylindrical case was similar with the exception that no consideration of collector strength was made. Details of these calculations will be presented in the final program report.

Figure 3-4 shows that the unvented sphere allows nearly the same fuel loading as the vented cylinder and is superior to the vented cylinder in specific power. This is shown in Figure 3-5 where specific power of the best converter designs are plotted against cell power. Figure 3-5 summarizes the geometry effect (Figure 3-3) and helium management consideration (Figure 3-4). The unvented cylinder is significantly lower in specific power to all other cases. Unvented capsules also reflect weight penalties into the aeroshell in the form of structure to limit thermal exposure and impact on the pressure vessel. A vented spherical geometry permits specific power from 5% to 10% higher than that of the best vented cylinder.

This difference is not sufficiently significant in vented capsule designs to warrant emphasis of spherical emitters (not yet fully reduced to practice) in place of the current-technology cylindrical configuration, as a component of the parametric generator study.

In general, unvented emitter designs do not exploit the performance potential of the Isomite converter based on other elements of current technology. Because considerable effort is being invested in the development of reliable venting mechanisms, it is assumed that no significant loss of credibility results if the parametric system study is based on a vented capsule design. Vented capsule technology for the Isomite converter should be available by the time

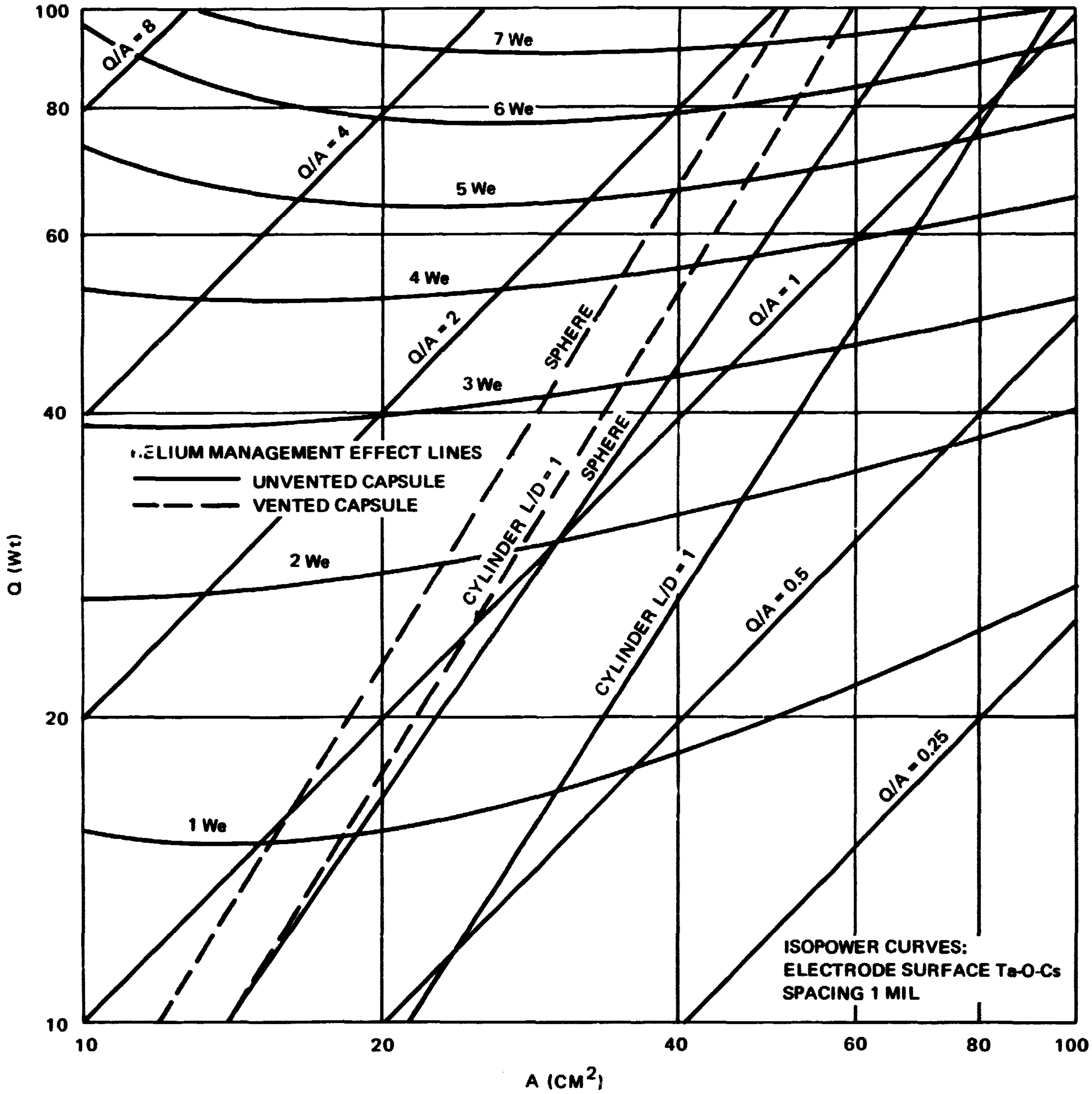

Figure 3-4. Effect of Helium Management on Fuel Load Limit Plotted on Q vs A Plane

70-1125

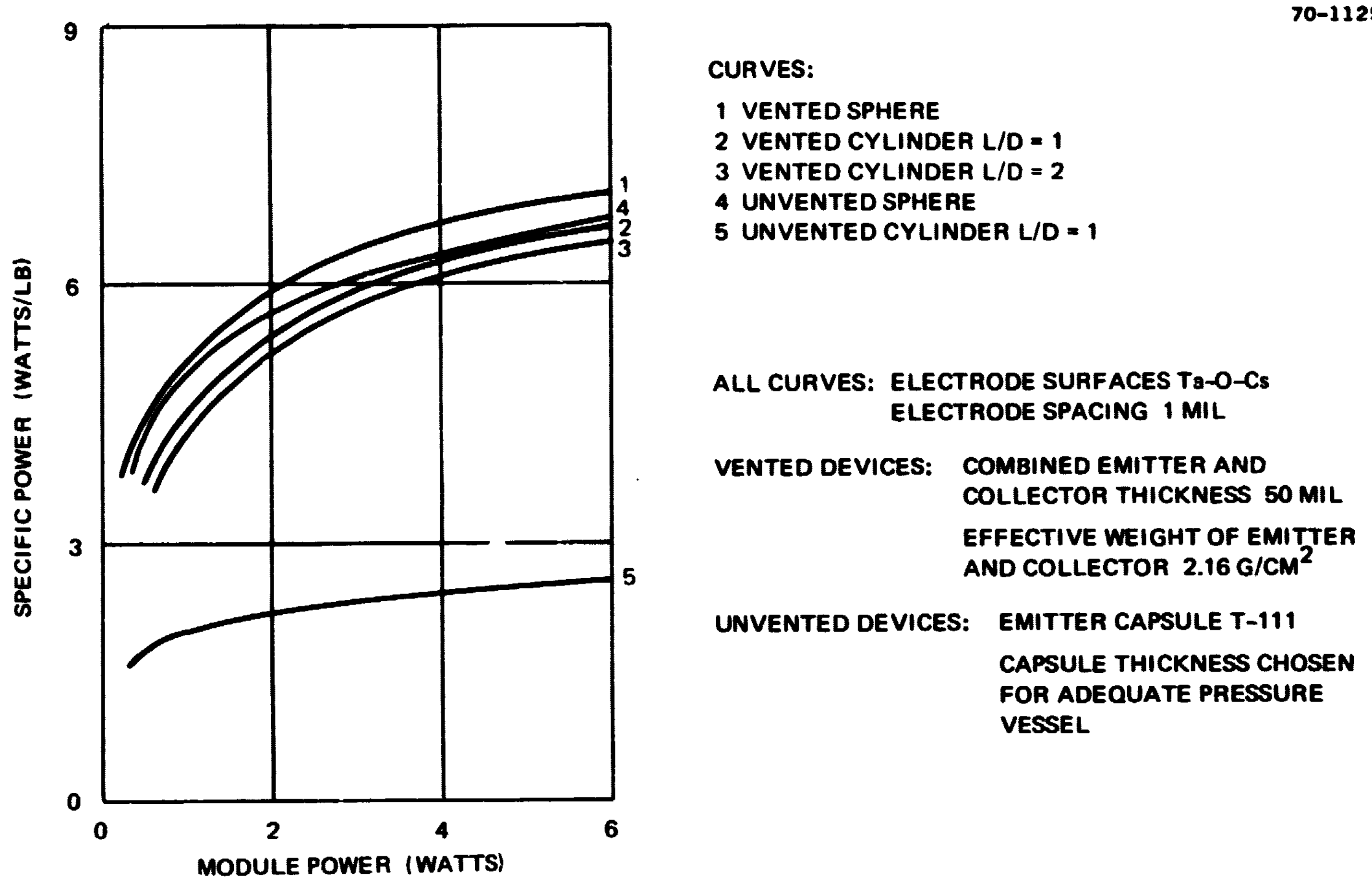

Figure 3-5. Converter Specific Power vs Module Power Showing Geometry and Helium Management Choices

development approaches flight qualification status. If, however, the credibility of a vented converter were in question, the unvented spherical capsule inside a cylindrical emitter would be a credible second choice contributing only a modest reduction in converter specific power.

BASELINE CONVERTER DESIGN

Parameter interactions discussed in Sections 2 and 3 establish baseline converter design and performance, which constrain elements of the system parameter study. The chosen baseline converter design has the following features to represent a credible combination of current and expected near-term technology.

1. Plutonia SSC fuel form
2. Vented cylindrical (L/D = 1) emitter geometry
3. Ta-O-Cs electrode surface system
4. One-mil electrode spacing
5. Total emitter and collector thickness of 50 mils.

Parametric system analysis in the following sections refers to this baseline converter. A brief future-technology review is included in Section 7 which considers system growth potential contributed by spherical electrodes, W-O-Cs surfaces, and high power density fuel forms.

PRECEDING PAGE BLANK NOT FILMED.

Section 4
CONVERTER SELECTION AND INTERCONNECTION

The choice of converter module size for the multicell generator is influenced by system interface and reliability requirements. A detailed reliability study is inappropriate for the Phase I parametric review. This section, therefore, considers a set of basic module selection criteria which act as boundary constraints for the reliability design of multicell generators having a specified range of output voltage. To accommodate converter failures design margin is introduced to provide a certain confidence level for achieving rated power output. Selection criteria are generated as a function of the number of converters (and hence module power level) required to provide power in a required voltage range with the highest confidence and minimum design margin.

To facilitate the reliability criteria review within the resource level of this effort, analysis is based on series-parallel electrical interconnection of a two-column converter array. This limitation of scope is generally consistent with the expectation that Isomite converters will have a lower open-circuit than short-circuit failure propensity, a situation promoted by the low temperature thermionic mode of operation in conjunction with close-spaced electrode systems. Because the purpose of series-parallel networks is to protect against catastrophic generator open-circuit failure by providing an alternate path for current in the event that converter open-circuit failures occur, two column arrays may be sufficient for devices with high open-circuit failure reliability. The present study would be enhanced by further consideration of other thermionic converter network configurations (References 17, 18, and 19). Derivation of results summarized in this section will be discussed in the final report.

RELIABILITY REQUIREMENTS

Reliability goals are tradeoffs between reliability and cost. EOL reliability guidelines assumed in this study to screen the number of converters required and the electrical interconnection are:

1. Generator reliability 0.99

2. Confidence level:

   Power output ≥ 50% EOL rated power 90%

   Power output ≥ EOL rated power 50%

These guidelines are generally consistent with typical requirements for unmanned space missions.

Mission failure is assumed to occur when generator power output falls below 50% of the design EOL power output. The primary mechanism for this event is a generator electrical open-circuit failure. Generator power output drops abruptly to zero when this occurs, followed shortly by complete failure upon discharge of the onboard secondary batteries. A high confidence level of 90% accompanies the reliability statement because of the catastrophic nature of this failure mode.

The primary mechanisms for failure to achieve the rated EOL power output are:

1. Excessive degradation of the thermionic converters.
2. Abrupt open-circuit or short-circuit failure of the tnermionic converters in excess of the number provided by the design margin.

Since failure to provide the required EOL power output usually only compromises the mission, a confidence level of 50% can accompany this generator reliability statement.

RELIABILITY DEMONSTRATION

DWDL experience with both research and production Isomite batteries indicates that a reliability demonstration test program should be oriented toward failure-free testing. While failures have occurred, their cause has been identifiable and corrected with appropriate design changes.

Figure 4-1 shows the number of failure-free converter qualification tests required to demonstrate a given converter reliability goal; these tests would be performed with final flight-type converters. Qualification tests do not distinguish between converter open-circuit and short-circuit reliability. In the absence of data, it is appropriate to assume that open-circuit and short-circuit reliabilities are equal. Accordingly, Figure 4-2 shows open-circuit reliability

70-1126

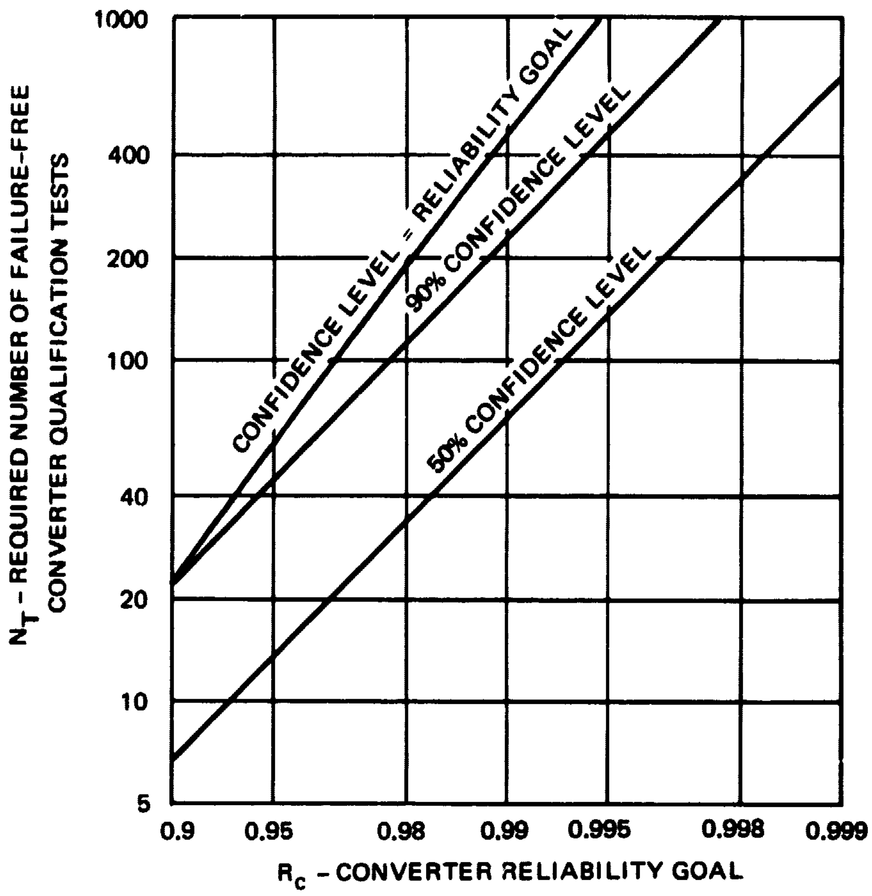

Figure 4-1. Converter Qualification Test Requirements

70-1127

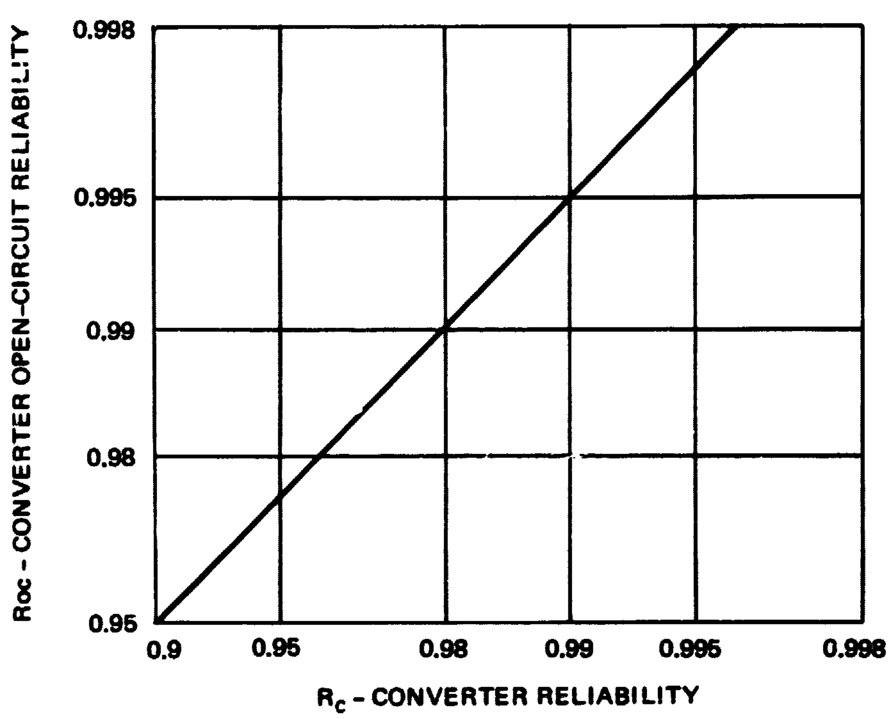

Figure 4-2. Converter Open-Circuit Reliability vs Overall Converter Reliability

as a function of converter reliability. Without data, a 50% confidence level should accompany this reliability statement. However, experience has shown that the open-circuit failure propensity is considerably less than that for short circuits. For purposes of this study, therefore, the open-circuit reliability statement shown in Figure 4-2 is retained but with an assumed 90% confidence level.

CONVERTER OPEN-CIRCUIT RELIABILITY REQUIREMENTS

Series-parallel electrical interconnection of a number of converters permits generator reliability to be considerably higher than converter reliability. Figure 4-3 shows a flat network array of converters composed of "c" and "r" rows. Three-dimensional networks have been reported (Reference 18) which suppress edge effects when failures occur. Networks with two or more series/ parallel connected columns reduce the probability of catastrophic generator open-circuit failure, because for this to occur, all converters in a given row must fail in open-circuit.

70-1128

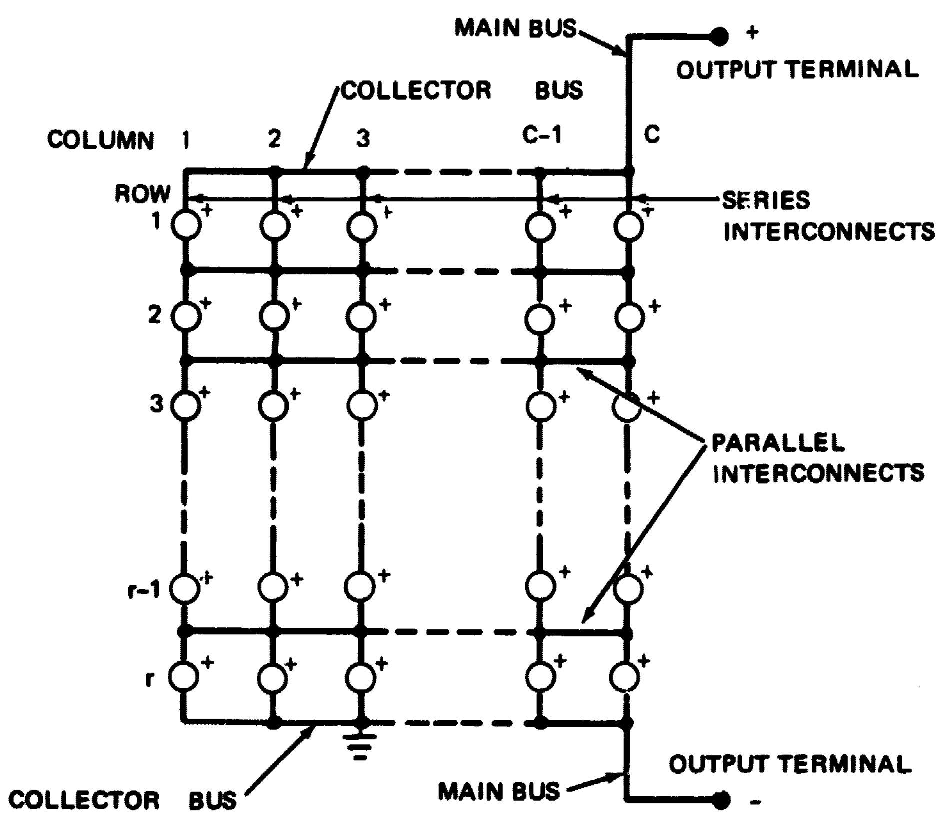

Figure 4-3. Generator Electrical Network

Figure 4-4 shows the converter open-circuit reliability requirements to achieve a generator reliability of 0.99. Generators containing up to 100 converters and four network columns are considered. Profiles are shown for a nominal converter output of 0.6 v, which represents the maximum cell voltage encountered in the current range of interest.

OVERALL CONVERTER RELIABILITY REQUIREMENTS

Overall converter reliability requirements are based on power loss considerations and the initial design margin required to compensate for potential converter failures. Figure 4-5 shows the initial generator design margin required to compensate for 1 and 2 converter failures with a two-column electrical network assuming negligible electrical connector resistance. Because converter failures are discrete events, the required design margin is larger in generators with fewer converters.

One converter failure is essentially equivalent to two converter failures, because the converter in the row adjacent to the failed converter is forced to

70-1129

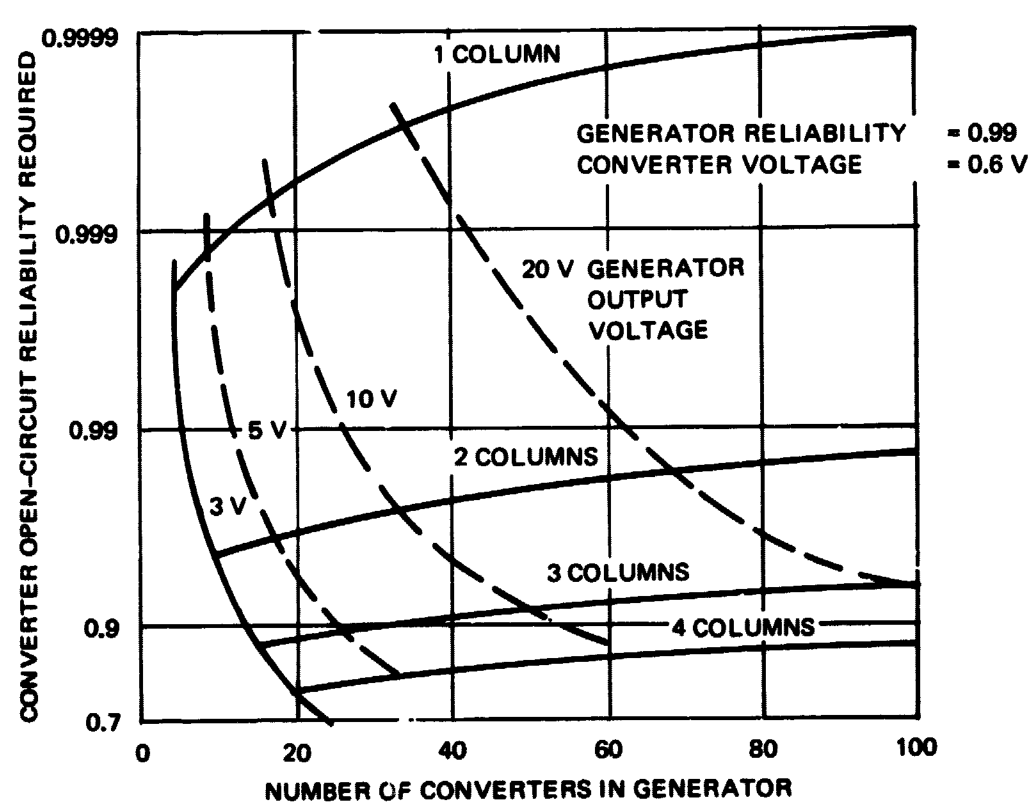

Figure 4-4. Converter Open-Circuit Reliability Requirements

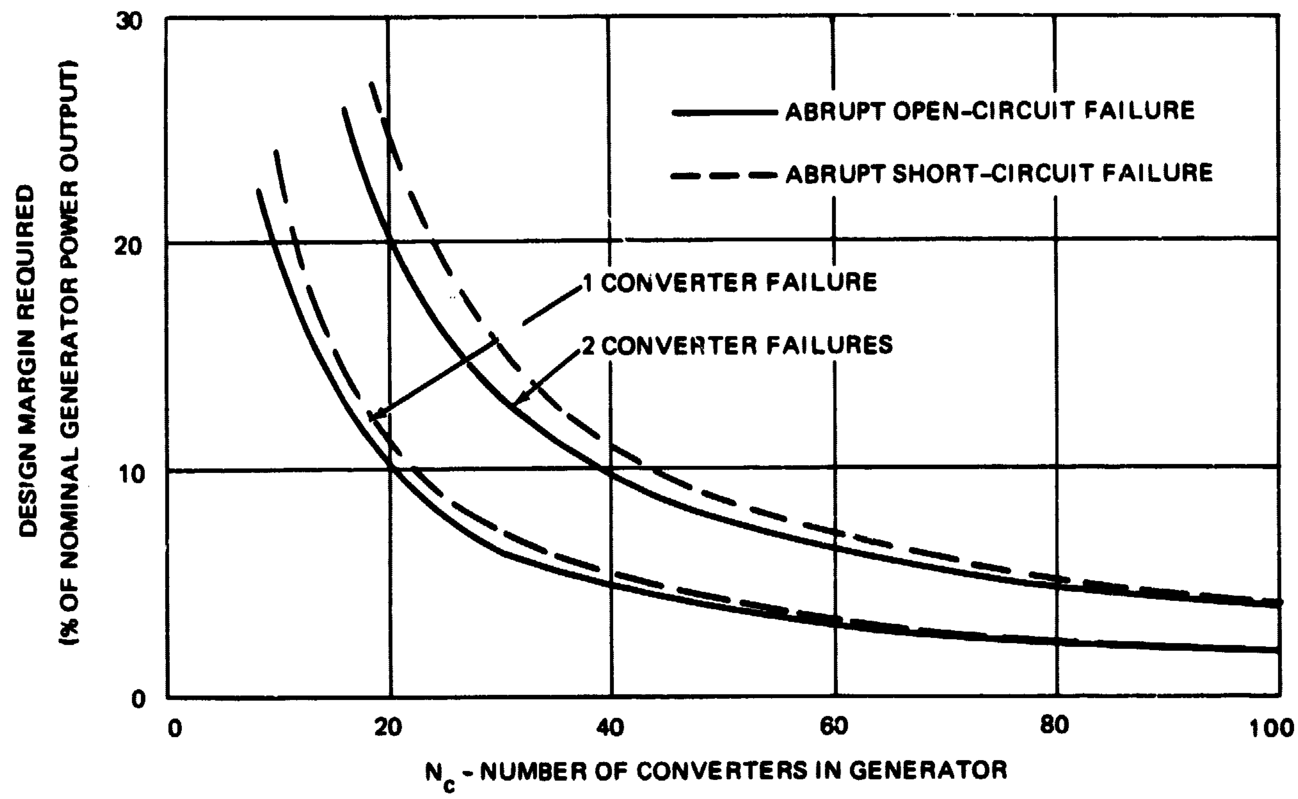

Figure 4-5. Generator Design Margin Required to Compensate for Potential Converter Failures (2 column electrical network: negligible connector resistance)

operate at either short-circuit or open -circuit (zero) current depending on the failure mode. Figure 4-5 indicates that the resultant power loss in a two-column network is essentially the same for both open- and short-circuit converter failures. Figure 4-6 shows converter reliability requirements at 50% confidence for up to two converter failures. These requirements are roughly comparable to the converter open-circuit reliability requirements with a two-column electrical network (Figure 4-4).

Figure 4-7 shows a parametric generator reliability summary. The generator open-circuit reliability requirement (derived from Figures 4-1, 4-2, and 4-4) is used as the criteria for determining the number of qualification tests required. In general, the number of failure-free qualification tests is on the same order as the number of converters in a generator. A two-column network is, therefore, an economically reasonable design goal. Figure 4-7 shows also the EOL power output confidence level as a function of number of converters for up to two converter failures.

70-1131

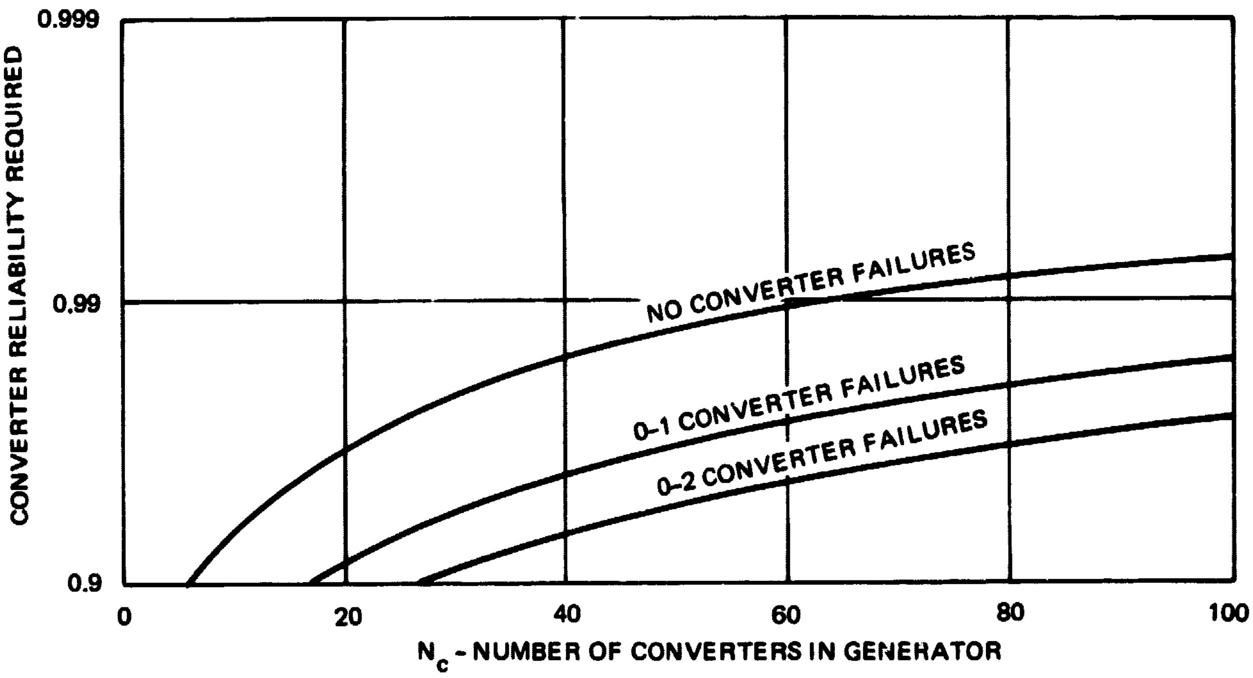

Figure 4-6. Converter Reliability Requirements at 50% Confidence Level

70-1132

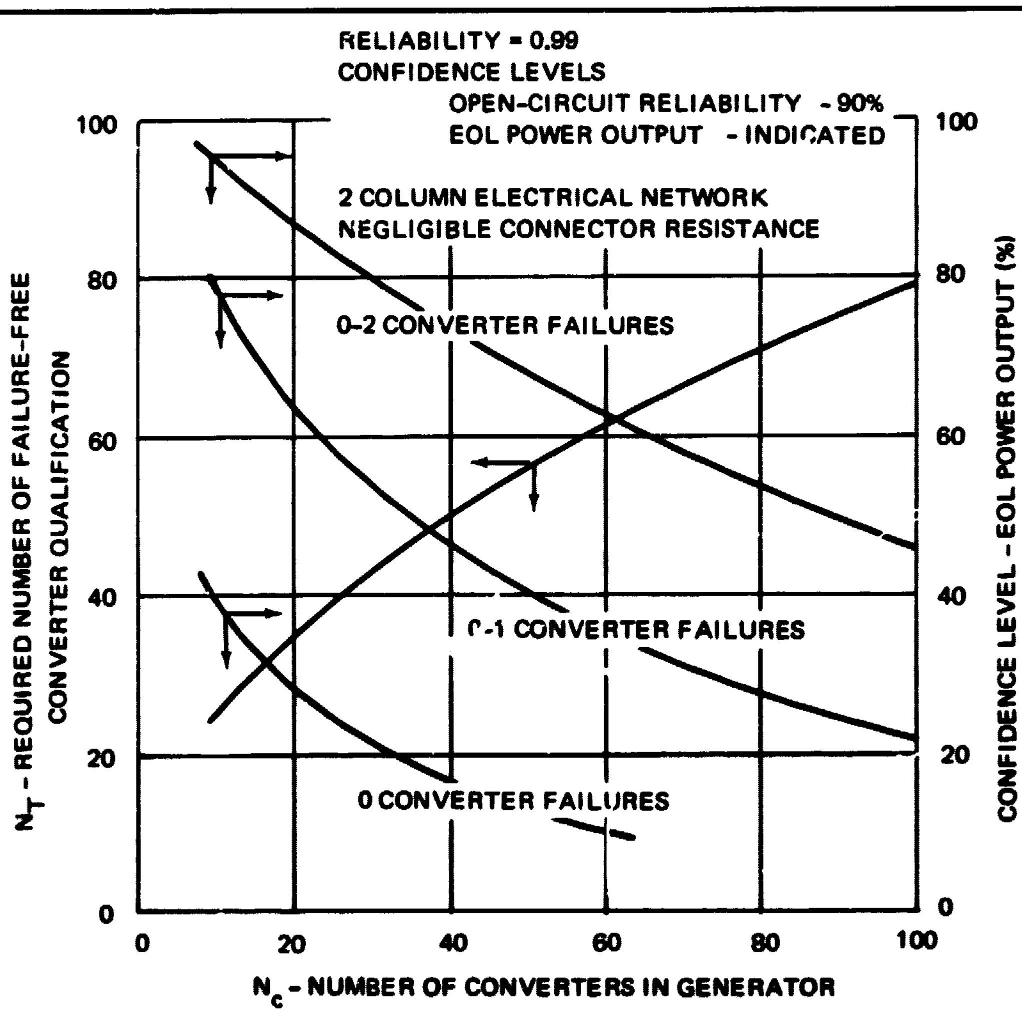

Figure 4-7. Generator Reliability Summary

Table 4-1 summarizes the range of design margin, EOL power confidence level, and output voltage for 50, 100, and 200 w_e generators composed of 1, 2.5, and 5 w_e baseline converters. Generator configurations shown in the "Design Selection" column generally meet the assumed reliability goals and have output voltages in the required range (3 to 10 v).

This section does not provide an exhaustive review of reliability design. However, the simplified analysis clearly provides converter selection criteria which accounts for basic reliability goals and constraints imposed by these goals on generator voltage. The results of this summary are discussed further in Section 7.

Table 4-1

GENERATOR DESIGN MARGIN AND VOLTAGE SUMMARY

Generator Power (w_e)	Nominal Converter Module Power (w_e)	Number of Converter Modules	Number of Failures	Initial Design Margin (%) (1)	EOL (2) Power Confidence Level (%)	Actual Converter Module Power (w_e)	Converter Terminal Voltage (v)	Maximum Generator Voltage (v) (3)	Design Selection
50	1	50	1	4.2	40	1.04	0.432	10.79	
			2	8.6	68	1.09	0.434	10.84	X
	2.5	20	0	0	28	2.50	0.482	4.82	
			1	11.2	65	2.78	0.490	4.90	X
	5	10	0	0	39	5.00	0.535	2.68	
			1	25	79	6.25	0.549	2.74	X
100	1	100	2	4.1	47	1.04	0.432	21.6	X
	2.5	40	1	5.5	47	2.64	0.486	9.72	X
			2	11.0	74	2.78	0.490	9.80	X
	5	20	0	0	28	5.00	0.535	5.35	
			1	11.0	65	5.55	0.541	5.41	X
200	1	200	4 (4)	4.1	47	1.04	0.432	43.20	X
	2.5	80	2	5.4	54	2.64	0.486	19.60	X
	5.0	40	1	5.5	47	5.25	0.538	10.76	X
			2	11.0	74	5.55	0.541	10.82	X

(1) For short-circuit failure (worse case than open-circuit failure)
(2) Generator reliability = 0.99
(3) Two-column network
(4) Provision for 4 failures necessary to reach ~50% confidence level

PRECEDING PAGE BLANK NOT FILMED.

Section 5
OFF-DESIGN PERFORMANCE

The performance of system-integrated converters may be different from the optimum characteristics reported in Sections 2 and 3 as a result of materials variability, aeroshell-imposed effects, mission power profile, and fuel decay during mission life. Power degradation under the influence of dominant variables is shown in Figures 5-1 through 5-6. Degradation which results from off-optimum values of ϕ_e, ϕ_C, ε, T_C, T_R, d, and R_L is plotted as P/P_o vs parameter/parameter$_o$ indicating the ratio of each component to its value if the converter were operating at optimum conditions. Figures 5-1 through 5-6 show power degradation as a function of parameter variability calculated for suboptimum cases of the subject parameter with all other

70-1133

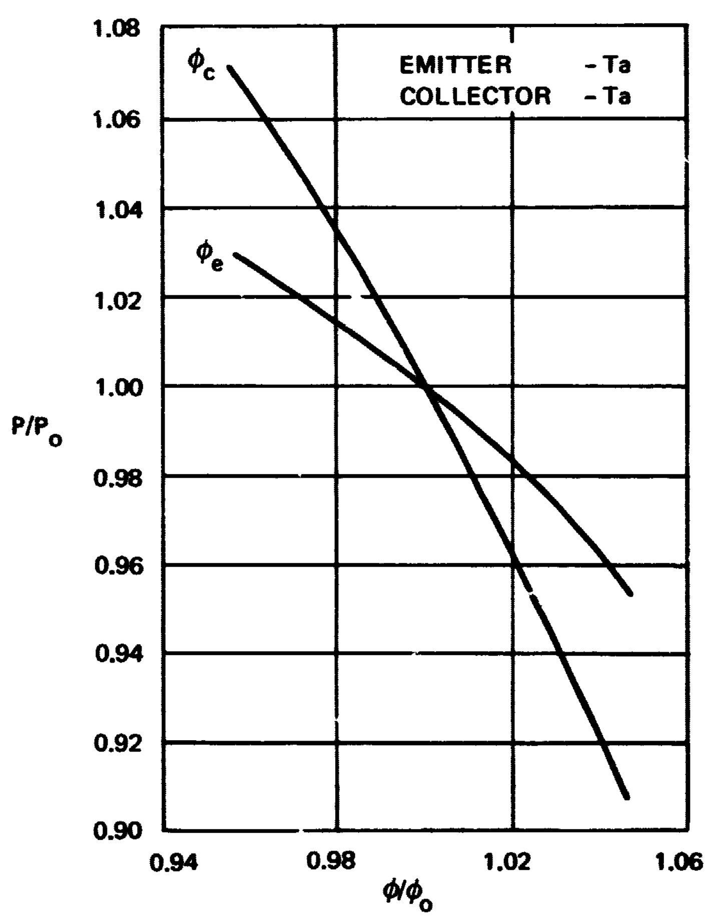

Figure 5-1. P/P_o vs ϕ/ϕ_o with All Other Parameters Constant

70-1134

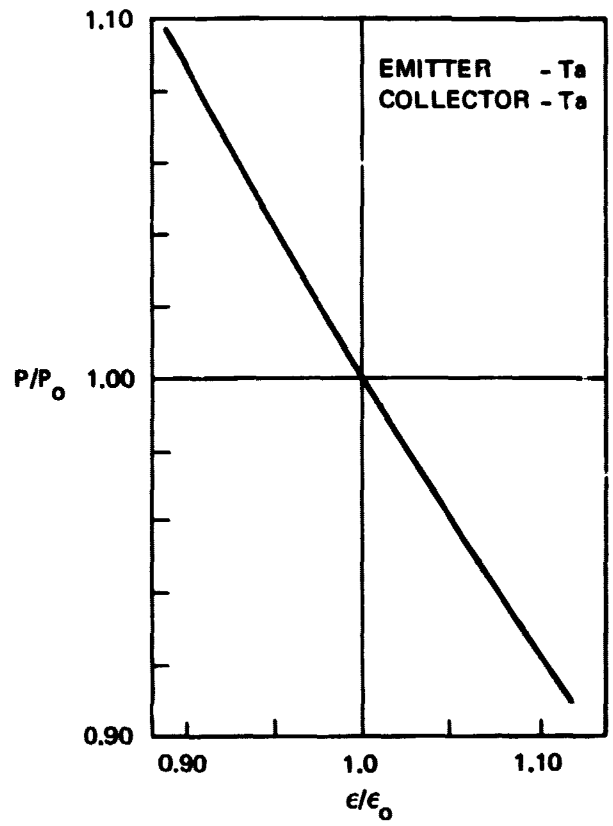

Figure 5-2. P/P_o vs ϵ/ϵ_o with All Other Parameters Constant

7:-1135

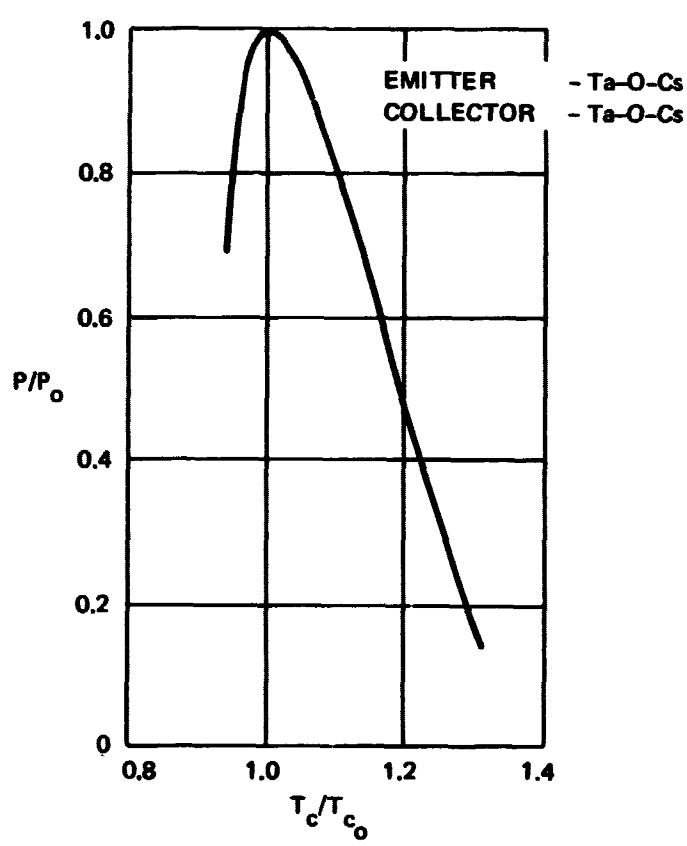

Figure 5-3. P/P_o vs T_c/T_{c_o} with All Other Parameters Constant

70-1136

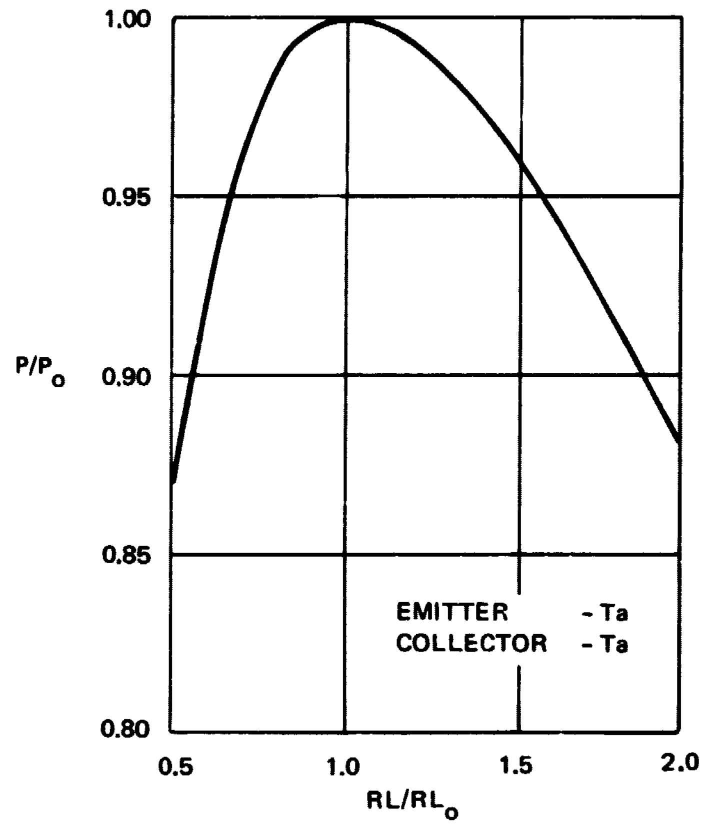

Figure 5-4. P/P_o vs RL/RL_o with All Other Parameters Constant

70-1137

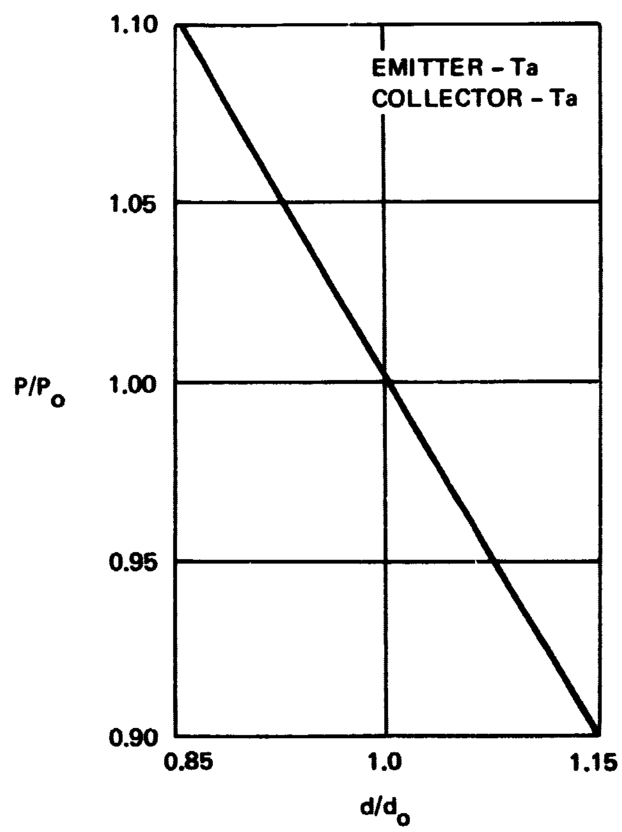

Figure 5-5. P/P_o vs d/d_o with All Other Parameters Constant

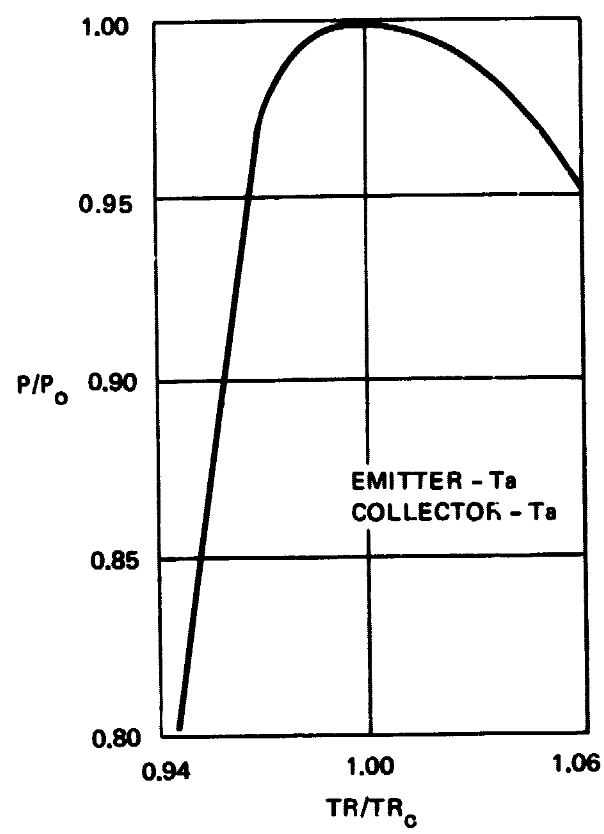

Figure 5-6. P/P_o vs TR/TR_o with All Other Parameters Constant

independent parameters input at previous optimum values. This review of performance degradation therefore, does not necessarily account fully for converter response in the conditions of the total mission environment or allow reoptimization of independent variables. The summary is useful, however, in showing the band widths (generally worst-case) of allowable parameter deviation from optimum which maintain converter power within 10% of its maximum value.

Figure 5-1 shows that variability of ϕ_c influences converter power in excess of twice the rate caused by a change in ϕ_e. A 5% to 8% variation in ϕ/ϕ_o produces a 10% variation in P/P_o. The influence of ε (Figure 5-2) is not as severe. However, decreasing ε produces a greater rate of increase in converter power than the rate of decrease produced by ε rising. Failure to optimize T_c has a significant influence on converter power (Figure 5-3). The curve describing $P/P_o = 0.9$ allows no more than a +7% to -4% change in T_c. The influence of T_c shown in Figure 5-3 is, however, the most extreme case because converters designed for a space mission will incorporate materials and construction features to reduce sensitivity to T_c. The least influential parameter is R_L (Figure 5-4) which can vary +85% to -55% before P/P_o falls below 0.9. It is assumed that this sensitivity to load resistance is reflected to the generator terminals and, therefore, describes an inherently small generator sensitivity to the load impedence. Electrode spacing and T_R have significant influence on converter output (Figures 5-5 and 5-6). The influence of T_R includes both an effect on electrode surface ϕ and changes in cesium vapor conductivity.

This parametric review does not allow T_e as an independent variable because it is inherent in the choice of electrode materials, T_c, T_R, and d. Figures 5-1 through 5-6 represent characteristics of converter module powers from 1 to 7 w_e to acceptable first order accuracy. The interaction of T_{co} with the thermal balance of the aeroshell is discussed in Section 7.

PRECEDING PAGE BLANK NOT FILMED.

Section 6
AEROSHELL DESIGN

The aeroshell structure (Figure 1-2) provides an operational housing for the converter array throughout mission life. The weight and specific power of the entire generator are largely determined by intrinsic converter characteristics (module size and power) and the aeroshell structure. Electrical connections (bus bars, leadthroughs, and connectors) and system integration hardware (shock mounts, mounting brackets, and attachment hardware) contribute generally small additional weight penalties. An important consideration is, therefore, optimum stacking of the converter array inside the aeroshell, which varies according to generator power and converter module selection. To facilitate this optimization, several aeroshell design constraints are assumed.

AEROSHELL BALLISTIC COEFFICIENT

The aeroshell vehicle is assumed to be constrained by a constant ballistic coefficient, selected as 30 lb/ft^2 on the basis of impact velocity and heating requirements. The impact velocity corresponding to this ballistic coefficient is just under 200 fps. Selection of the ballistic coefficient (β) involves an optimization process. An increase in β means a size and weight reduction for the flare but an increase in ablation, insulation, and impact structure requirements. A preliminary study of these tradeoffs indicates that ablator and insulator thicknesses increase approximately as the square root of β, while the flare weight decreases inversely with β. Minimum weight occurs when the ballistic coefficient is maximized to the point where it is governed by impact considerations. The present assumed value of β (30 lb/ft^2) is conservative for impact survival. Impact tests of simulated cylindrical Isomite converters (Reference 20) indicate that unprotected devices can survive impact on granite at velocities exceeding 200 fps. In the space mission configuration, converters are protected by the aeroshell and crush-up structure, which is designed to absorb a major portion of the impact energy. Furthermore, the loose packing of cells within the aeroshell will enable the devices to absorb energy by compacting.

NUCLEAR SAFETY IN LAUNCH PAD ABORT CONDITIONS

The combination of aeroshell structure and multicell array presents an attractive system for safety in a launch pad abort environment. Although the aeroshell will absorb impact forces, the primary containment structure is contributed by the emitter and collector layers. A thin platinum layer around the fuel liner prevents high temperature oxidation and is protected against impact by the collector. A platinum layer (of equal thickness) around the aeroshell would be more weight efficient, but direct thermal contact with the fuel would be lost. A platinum layer on the aeroshell would also be more vulnerable to impact penetration. Platinum is incorporated in the converter with negligible weight penalty, because it can be used as a component of the emitter capsule.

Analysis (Reference 21) shows that typical plutonia fuel containers clad with platinum will survive the currently most severe chemical propellant fires, provided that good thermal coupling is maintained with the fuel. This is because melting, not oxidation or thermal shock, is the prime concern. Platinum has almost negligible corrosion rates in contact with sea water, air, soil, and many other materials. The 20-mil design thickness is conservative for corrosion protection.

REENTRY, IMPACT, AND BURIAL

Design and safety requirements for the generator assumed in this analysis are presented in Table 6-1. Reentry envelope conditions extend to super-orbital reentry. Figure 6-1 shows the effect of these conditions on the type of trajectory attained. For the maximum velocity criterion of 36, 300 fps, there are only two possible trajectories. One is the multi-elliptical orbit reentry with the body grazing the earth's atmosphere until final reentry. The second is a prompt, immediate trajectory.

Selection of the worst case reentry conditions depends upon the accident analysis of a given mission. For a large class of planetary missions where earth departure velocity exceeds 36, 300 fps, the escape boost from earth orbit can be programmed at shallow exit angles (<4°). Failure after 36, 300 fps at these angles results in hyperbolic trajectory and no reentry (Figure 6-1). There is a low probability of powered off-course maneuvers which lead to eventual failure and reentry. For the purposes of this study, therefore, the upper limit of reentry velocity can be fixed at 36, 300 fps.

Table 6-1

SAFETY CRITERIA AND GUIDELINES

Safety Criterion	Guideline
Fuel release	None under normal or credible accident conditions
Minimum design life	12 yr (10-yr mission)
Intact reentry	Including impact and partial earth burial
Impact at terminal velocity	Intact impact on granite
Partial earth burial maximum temperature	2500°F (1644°K)
Hydrostatic water pressure	Sufficient to limit ocean surface contamination below 10^{-2} MPC
Corrosion life	10 half-lives
Reentry velocity	36, 300 fps (max)
Reentry angles	All prompt reentry trajectories
Launch-pad explosion	10, 000 psi static overpressure 10, 000 ft-lb debris energy
Launch-pad fire	Liquid chemical propellant

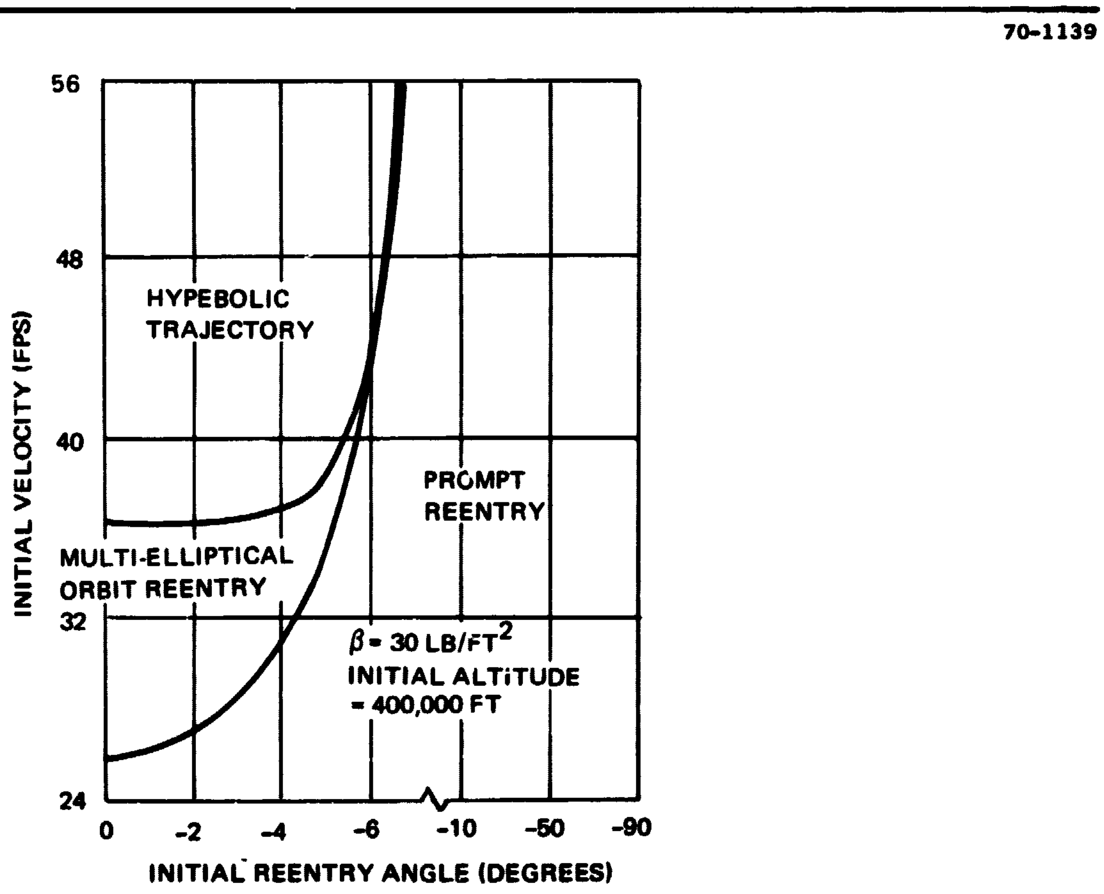

Figure 6-1. Envelope of Reentry Conditions

For the reentry vehicle with a fixed ballistic coefficient, graphite ablator thickness requirements can be ascertained from worst-case trajectory heating and pressure transients. Previous studies of graphite-protected radioisotope heaters (Reference 21) show that the worst prompt trajectory for graphite ablation and internal temperatures occurs at the shallowest prompt entry angle. At maximum velocity, this angle is -5.2° as shown in Figure 6-1.

The aeroshell configuration is favorable to limit penetration and complete burial on land impact. The blunt shape presents a low impact loading which will not bury the vehicle as a whole to a significant depth in typical soil conditions. This conclusion is based on the penetration analysis reported for a spherical body of similar size (Reference 22). The aeroshell structure is not expected to be breached on land impact because of the low impact velocity and crushup material. In the unlikely event that converters spill out after impact, each is fully protected against corrosion by the platinum layer. For the power levels considered, no temperature problem exists for individual converter burial, even in soil of low conductivity.

THERMAL DESIGN ASSUMPTIONS

Trajectory and aeroheating data are available from previous studies (Reference 21) to estimate the amount of graphite ablation at the stagnation region. A POCO graphite thickness of 0.5-in. is sufficient, with a safety margin of about 1.3, to protect against all prompt reentry trajectories up to 36,300 fps. Thickness requirements around the nose, on the sides, and on the flare, are determined using Newtonian flow theory. About 0.15 in. is provided on the sides; 0.25 in. is provided on the flare section.

Insulation requirements depend in large measure on the material type, heat treatment, and density of insulator selected. On the nose section, severe heating and high thermal impedance requirements dictate selection of an insulator such as pyrographite. On the sides, reentry heating is less severe and normal operating temperature considerations are more important. A moderate impedance insulator such as aluminum oxide, reinforced pyrographite, or fibrous graphite could be used. For the Phase I analysis, the density of all insulation was assumed to equal that of POCO graphite. A thickness of 0.1 in. was assumed along the cylindrical sides and on the flare. Reentry temperatures can be minimized by provision of copper "shoes" brazed to the cells and inside the aeroshell; provision is made to electrically isolate converters from the shell structure. The copper provides good heat transfer during normal operation but melts on reentry reducing thermal contact. Titanium is assumed in this analysis for the aeroshell and flare structural material because of its light weight, moderately high melting point, and good strength. Impact data also exist for titanium structures (Reference 23) which categorizes this material with 4130 steel. A titanium thickness of 0.03 in. is assumed throughout.

CONVERTER ARRAY CONFIGURATION

Converters may be arranged within the ellipsoidal-ended housing in two possible stacking arrangements. One is mating the flat ends of the cylindrical cells to the inner curved surface of the housing. The second is coaxial stacking with curved surfaces of the converters parallel to the inner curved surface of the housing. It can be shown, for cylindrical converters with $L/D = 1$, that coaxial stacking is the optimum packing arrangement (minimum wasted space) In the analysis, coaxial stacking is assumed throughout.

For a given total generator power and a given cell size, there are various coaxial stacking arrangements. Figure 6-2 shows the internal cross-sectional area of the housing per cell for a 5-w_e module and selected radial groups. This curve shows that an arrangement of four or five cells around the circular cross-section of the housing results in optimum stacking. A greater number of cells around the circumference, assuming no internal cells, results in more wasted space. Conversely, a stacking of two or three cells does not result in as dense a packing as four or five cells.

A design weight analysis for spherical and cylindrical shapes (Reference 24) shows that for a given volume, the optimum length of a cylinder to attain minimum weight occurs when $L_a/D_a = 1$. On the other hand, a preliminary pressure distribution analysis based on Newtonian flow theory, indicates an L_a/D_a close to 2 ensures aerodynamic stability. Therefore, optimum weight will occur for the reentry vehicle when converters are arranged in radial groups of 4 and 5 with enough rows to give an aeroshell L_a/D_a between 1 and 2.

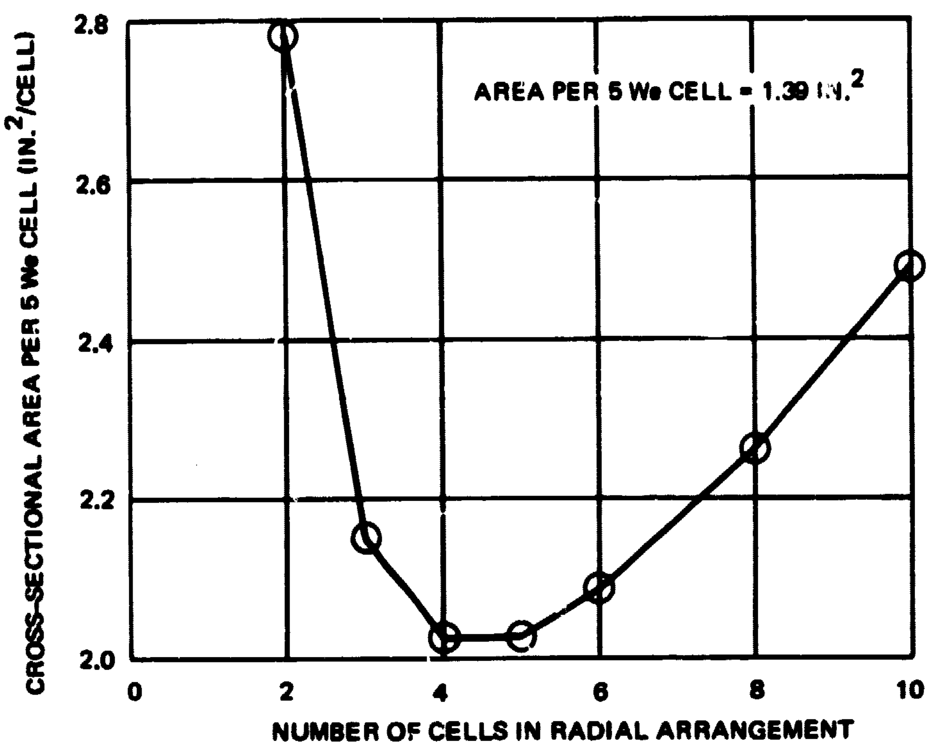

Figure 6-2. Packing Density of Circular Cells in a Circle

To explore the weight parametrics with different cell stacking options, a DWDL computer program was used to calculate the total generator weight including reentry vehicle with a constant ballistic coefficient of 30 lb/ft^2. In this program, individual cell dimensions and power are input and reflect the baseline design described in Section 3. For all practical combinations of columns around the aeroshell circumference and up to 200 w_e total power, the program solves the total system weight and resulting normal operating temperature at the graphite surface assuming radiation to space at a constant emissivity of 0.8 (Reference 25). The code starts with three columns and takes a progressive number of rows until 200 w_e is reached. The process is iterated for a greater number of columns. Details of the iterative weight analysis will be discussed in the final report.

AEROSHELL DESIGN OPTIMIZATION

Using the computer program, generator design and weight characteristics were determined for four module powers (1, 2.5, 5, and 7 w_e) of the baseline design (Section 3). These converters are characterized by Ta-O-Cs surfaces with 1-mil spacing, vented cylindrical emitter geometry (L/D = 1), and plutonia SSC fuel. Diameters (including 10 mils for electrical insulation), lengths (with 0.5-in. clearance for helium vent tubes), thermal powers, and converter weights are inputs to the code. All possible combinations of number of columns (between 3 and 20) and number of rows (between 1 and 20) corresponding to generator powers to 200 w_e are calculated. Some combinations result in generator L/D ratios less than unity which are considered unacceptable for reentry vehicle design for reasons previously discussed.

Specific powers for the various combinations are plotted against total generator power in Figure 6-3 for four module powers. Solid curves show the maximum specific power attainable at any given generator power level. Spacing of the data bands illustrates a monotonic increase in specific power with module power, the rate of gain diminishing in the 5 to 7 w_e power range.

This analysis neglects a basic requirement to match T_{rad} and T_{co} allowing for a temperature differential across the layered structure of the aeroshell. Figure 6-4 shows T_{rad} for optimum converter stacking and T_{rad} required by optimum T_c values plotted as a function of generator power for cell power from 1 to 7 w_e. Only single coincidences of T_{rad} actual and required values occur for any module power. There is no natural matching of temperatures for the 1-w_e module or any module powers in generators greater than 100 w_e. Significantly lower values of T_{rad} can be obtained by off-optimum stacking configurations with (at high generator powers) an attendant slight decrease in specific power.

This integration problem may be solved by iterative selection of both T_{rad} and T_c for a range of off-optimum cases, to search for a maximum specific power generator. It is recommended that the Phase II design study incorporate this approach.

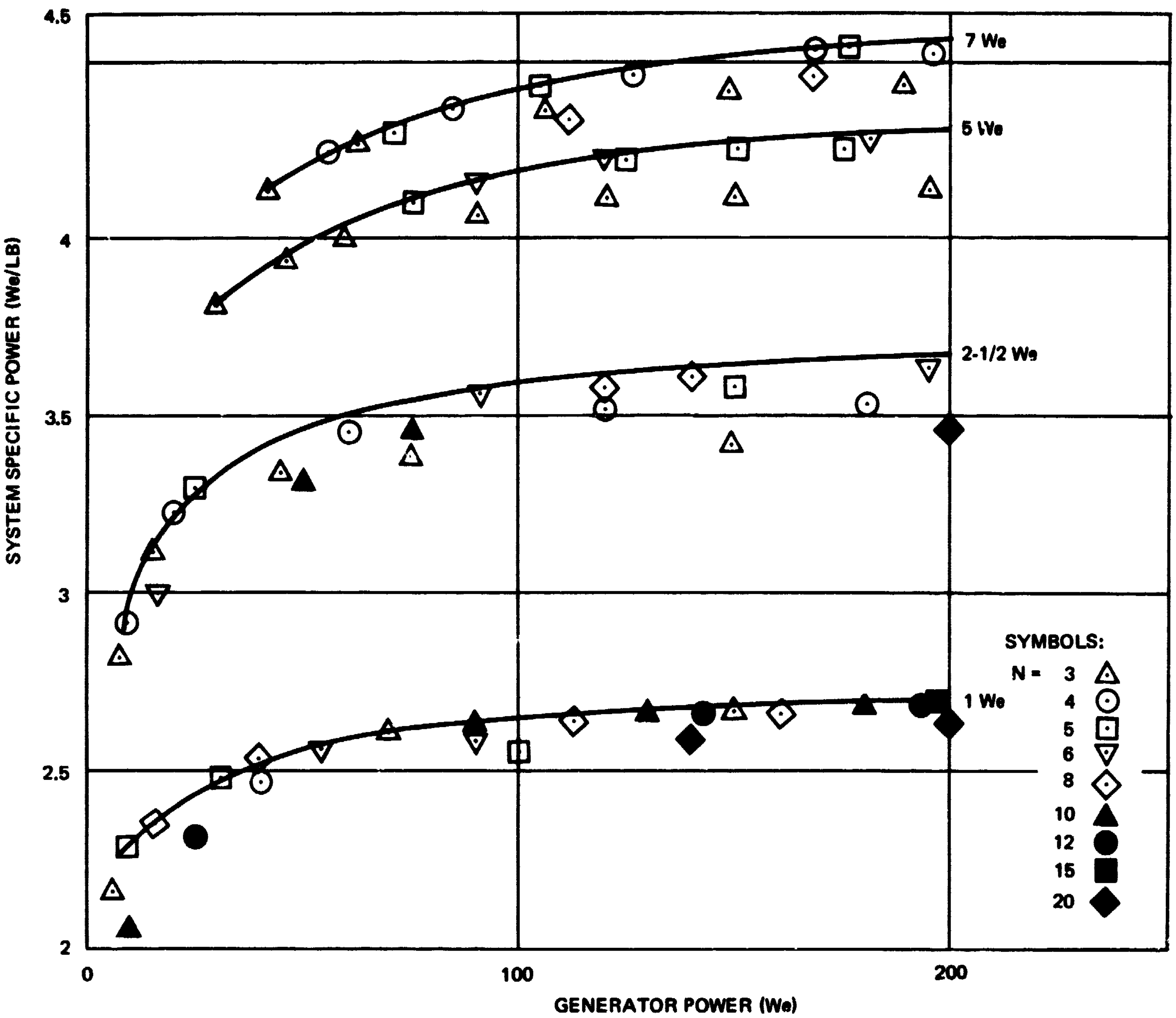

Figure 6-3. System Specific Power vs Total Generator Power for Selected Cell Powers

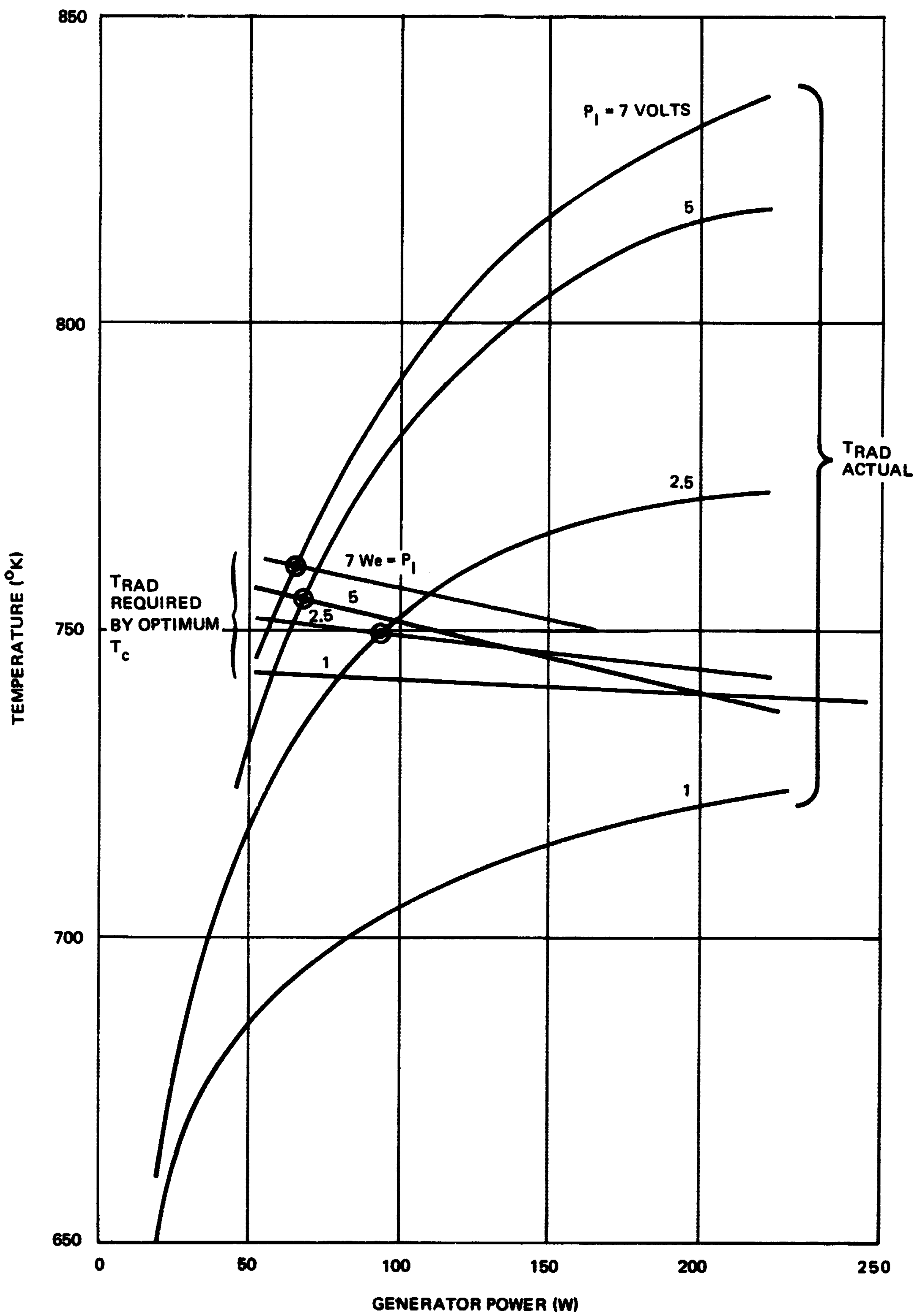

Figure 6-4. Actual T_{rad} and T_{rad} Required by Optimum T_c vs Generator Power for Different Module Powers

Section 7
GENERATOR CHARACTERIZATION

Preceding sections discussed the principal components of a multicell generator design and identify a parametric range of interest for dominant constraints. Generator characterization is achieved by summary description and integration of system components.

In general terms, this analysis shows that current-technology thermionic multicell space power generators in the 50 to 200 w_e power range theoretically can achieve specific power between 2.5 and 4.5 w_e per lb and efficiencies from 6.25% to 7.4%, depending on converter size and generator power. Generator specific power shows plateaus characteristic of each converter module size. Module power of 1 and 7 w_e bracket the specific power range 2.5 to 4.5 w_e/lb respectively, with a corresponding range of efficiency. In practice, the weight of system integration structure and electrical connection losses reduce these values slightly.

SYSTEM INTEGRATION OF AEROSHELL ASSEMBLY

Mechanical and electrical integration components are required to attach the aeroshell assembly to the space vehicle, provide reentry separation, and bring the electrical output to convenient terminals. Figure 7-1 shows a typical method for mounting the generator on the vehicle structure. Mountings are sized to isolate a 50 lb aeroshell structure from vehicle-imposed shock and vibration conditions of 100 g for 4.5 ms and 20 g from 0 to 2000 Hz, respectively. Table 7-1 summarizes mounting component weights.

Electrical connection losses decrease with increasing generator voltage. Figures 7-2 and 7-3 show parametric characteristics of the electrical leads, assuming OFHC (oxygen-free high-conductivity) copper for the lead material. OFHC copper is chosen for its high efficiency, low vapor pressure, and high ductility. High ductility minimizes interconverter mechanical load transmission resulting from thermal expansion and launch loading effects. Lead

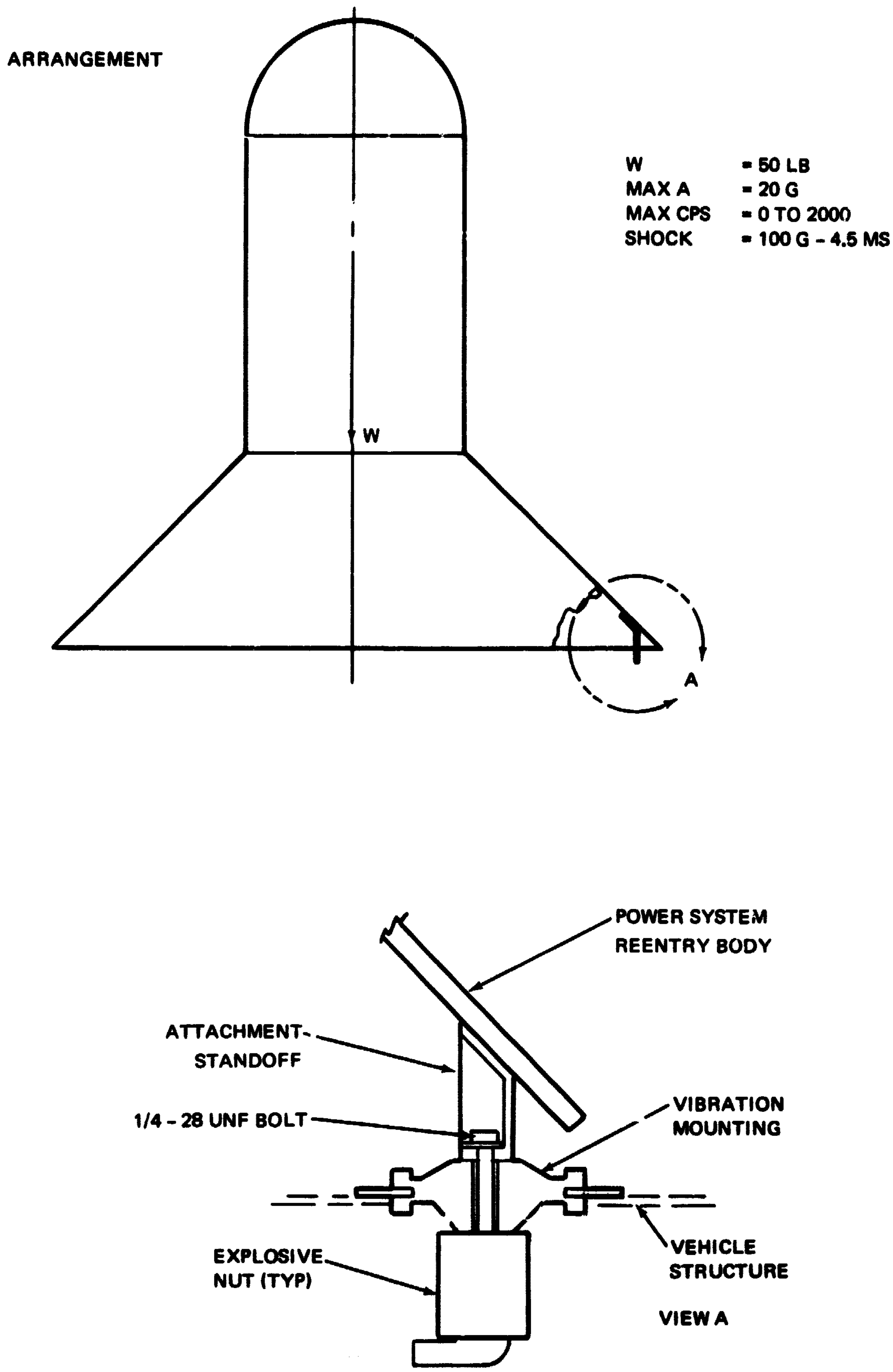

Figure 7-1. Vibration Mount for Multicell Generator

Table 7-1

MOUNTING AND SEPARATION SYSTEM WEIGHTS

Component	Source	Quantity	Unit Weight (lb)	Total Weight (lb)
Attachment Standoff	(1)	4	0.15	0.60
Vibration Mounting	(2)	4	0.31	1.24
Explosive Nut	(3)	4	0.30	1.20
Mounting Bolts	(4)	4	0.04	0.16
Total Weight				3.20

(1) Standard forged aluminum fitting
(2) Standard HT series mounting, Lord Mfg. Co.
(3) Space Ordnance Systems
(4) Standard 12-pt high strength 1/4-28 UNF bolt

70-1144

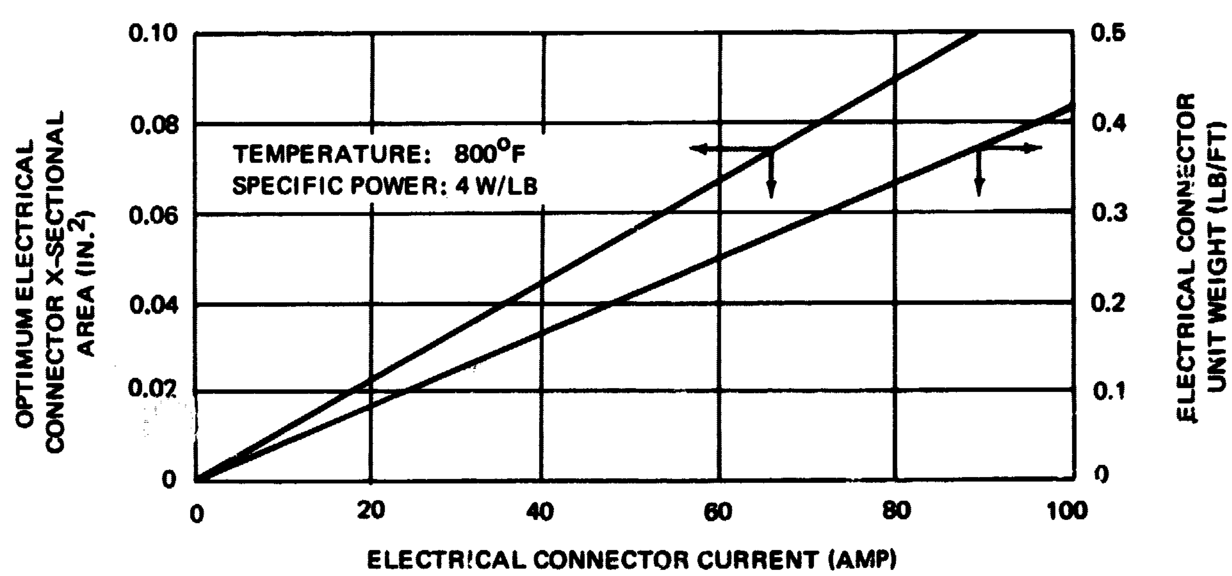

Figure 7-2. Connector Sizing

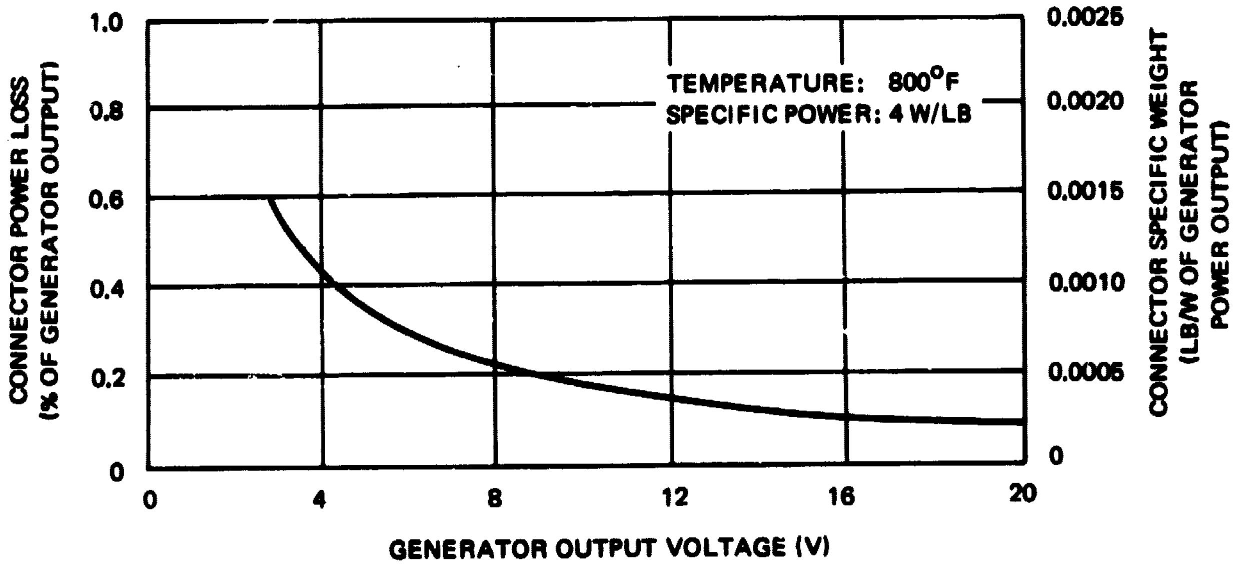

Figure 7-3. Connector Characteristics Per Foot of Effective Length

optimization may be expressed in terms of overall generator specific power and voltage. Details of the analytical method will be discussed in the final report.

Figure 7-2 shows minimum weight connector sizing data for a nominal generator specific power of 4 w_e/lb. Except for the parallel interconnects (Figure 4-3), the cross-sectional area of all electrical connectors is established by current flow, independent of connector length. In generator electrical networks containing three or more columns, relatively high-resistance parallel interconnects may be used to minimize power loss from converter short-circuit failures.

Figure 7-3 shows connector power loss and weight characteristics as a function of generator output voltage, per foot of effective connector length. The effective connector length may be determined approximately by summing:

1. Main bus lengths
2. One-half of collector bus lengths
3. Total length of series interconnects in one column

The collector bus carries, on the average, one-half the generator current. Because current divides proportionally among the columns in the generator, series interconnector weight is proportional to generator power output and current but is essentially independent of the number of columns in the generator. The multicell generator configuration is compact, and therefore, the main bus connecting the generator to the power converter can be expected to contribute the predominant weight and power loss which are, in any case, small and typically less than 1% of generator weight and power output, respectively.

GENERATOR RELIABILITY AND VOLTAGE

Section 4 shows that generator voltage cannot be optimized independently of the reliability requirements. Figure 7-4 shows generator specific power as a function of generator voltage, accounting for the effect of design margin. These curves are constructed from data in Table 4-1 for generator configurations with an acceptable EOL power confidence level (~50%). Specific power is scaled from data in Figure 6-3 by adding weight for design margin components.

70-1146

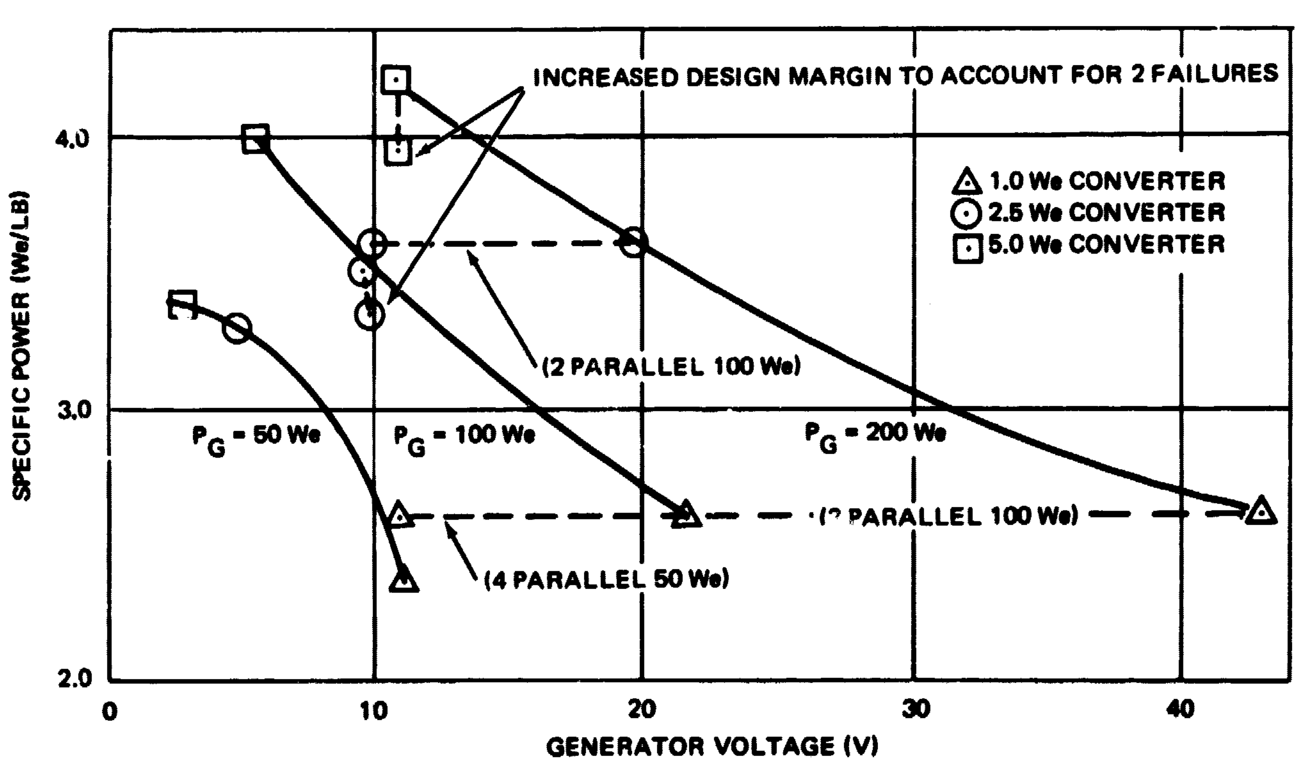

Figure 7-4. Generator Specific Power vs Generator Voltage with Generator Power and Converter Power as Parameters

Figure 7-4 shows that there is no optimum voltage for any generator power and that increasing voltage is gained at the expense of generator specific power. Generators composed of 5 w_e modules have the highest specific power in all cases, including the 50 w_e generator, when a 25% design margin is required to meet reliability criteria. The 5 w_e module is superior to lower power modules in 100 and 200 w_e generators when additional design margin is allowed for a second converter failure. The 50-w_e generator composed of 5-w_e modules has only marginally acceptable voltage for optimum converter conditions. However, Figure 5-4 shows that a change in R_L of 10% causes a negligible change in P_o and therefore converter operation slightly off-optimum could be used to increase generator voltage to a 3-v minimum level. The 5-w_e converter also provides economic benefits in the form of fewer converters per generator and therefore fewer failure-free converter qualification test to demonstrate required generator reliability.

SELECTION OF CONVERTER POWER

The general trend of specific power in Figure 6-3 shows a diminishing rate of gain for generators composed of modules in excess of 5 w_e. A 5-w_e module size is also the largest which satisfactorily meets the reliability/ voltage requirements of a 50 w_e generator. The 5-w_e size therefore appears to be the best module choice for all generators in the range of interest.

With 5 w_e modules, T_{co} is incompatible with T_{rad} near minimum weight aeroshells for generators larger than 65 w_e. Corrective measures generally involve additional weight penalties in the form of an enlarged aeroshell, radiator fins, or off-optimum converter operation. Estimation of the best solution is part of the Phase II study. However, a worst-case screening test shown in Figure 7-5 indicates the 5-w_e module continues to provide a superior specific power level. Figure 7-5 compares generator specific power corresponding to optimum converter operation with that provided by converters operating at off-optimum T_c (Figure 5-3) to match the required aeroshell T_{rad}. The specific power degradation at the 200 w_e level is probably exaggerated by the single-solution remedy. In Phase II, tradeoffs between increasing aeroshell area and operation of off-optimum T_c will be evaluated. It is anticipated that above P_g of 100 w_e, system specific power provided by the 5-w_e module will continue to be approximately 4 w_e/lb after all design contingencies are accounted for.

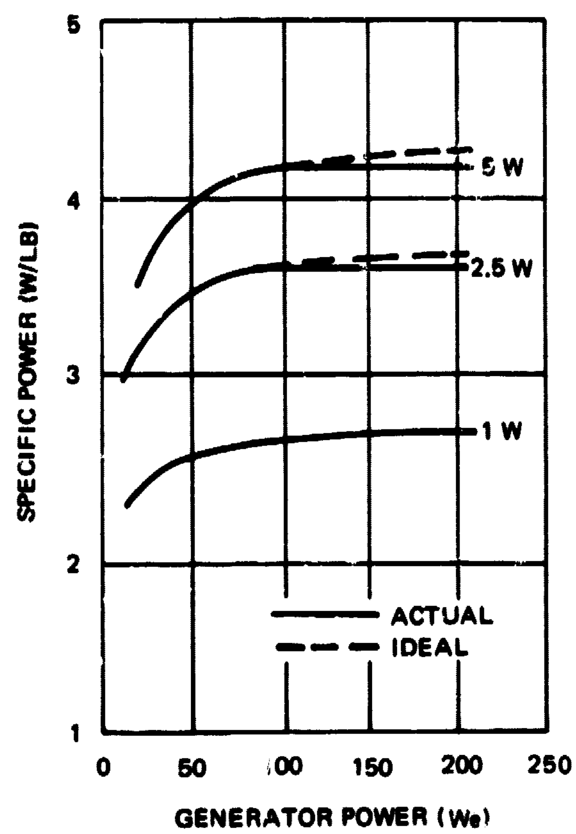

Figure 7-5. Worst-Case Degradation of Specific Power to Allow for Matching T_c with T_{rad}

GENERATOR CHARACTERIZATION

Table 7-2 summarizes characteristics of nominal 50, 100, and 200 w_e multicell generators composed of baseline 5-w_e modules. Nominal EOL generator power is considered the rated power of the generators. Characteristics account for fuel decay to the end of a 10-year mission, design margin required to provide a 50% confidence level for EOL power rating, and an estimation of weight penalties contributed by electrical connections and aeroshell mounting devices. The matching of T_c and T_{rad} is assumed at no penalty in converter efficiency or weight; the Phase II study will refine this estimation.

Table 7-2 shows that the system integration structure slightly degrades nominal specific power. Allowances for design margins, however, contribute a noticeable reduction in overall efficiency compared with inherent converter efficiency. This effect is especially noticeable for the nominal 50 w_e generator where efficiency is reduced from 7.25% to 5.9%.

Table 7-2

50, 100, and 200 W_e GENERATOR DESIGN SUMMARY

Characteristic	Nominal EOL Generator Power 50 w_e	100 w_e	200 w_e
Aeroshell inner diameter (in.)	3.23	3.62	4.84
Aeroshell cylindrical length (in.)	5.02	6.86	8.70
OD generator system (in.)	3.79	4.18	5.40
Flare diameter (in.)	9.53	12.12	16.90
Ballistic coefficient (lb/ft^2) (1)	30	30	30
Radiative surface temperature (°K)	749	779	818
Approx ΔT, across insulation (°K)	23	27	39
Converter efficiency (%)	7.25	7.25	7.25
Weight summary (lb)			
Isomite converters	9.24	15.40	30.80
Cylinder			
Ablator	1.25	1.70	2.81
Insulation	0.75	1.02	1.69
Crushup	0.20	0.26	0.46
Impact plate	0.08	0.10	0.18
Copper shoes	0.25	0.42	0.84
Aeroshell	0.38	0.54	0.94
Flare			
Structure	0.56	0.95	1.87
Insulation	0.49	0.83	1.65
Ablator	1.57	2.65	5.26
TOTAL	14.77	23.87	46.50
Nominal specific power (w_e/lb)	3.39	4.19	4.30
Generator voltage (v)	2.74	5.41	10.82
Generator current (amp)	18.25	18.50	18.50
Connector power loss (w_e)	0.5	0.3	0.16
Electrical connector weight (lb)	0.1	0.12	0.15
Aeroshell mount weight (lb) (2)	1.24	1.24	1.24
Overall efficiency (%) (3)	5.9	6.6	6.6
Overall specific power (w_e/lb)	3.10	3.96	4.18
Dose rate at 10 ft from center axis (mrem/hr) (4)	10 [5 (5)]	16 [8 (5)]	30 [14 (5)]

(1) Design requirement
(2) Shock mounts only charged to generator
(3) Allowing for design margin and connector loss
(4) Calculated at 5 years into mission for current grade PuO_2 (1.2 ppm Pu-236 and 10^4 sec-neutrons/sec-g Pu-238)
(5) Near future available PuO_2 fuel grade

The assessment for the mounting structure has been limited to shock and vibration isolation because no data exist describing the survival of Isomite converters in the mission shock and vibration environment. This weight penalty is therefore a reasonable component of the generator system. Because the use of attachment structures and release devices is dictated by vehicle design requirements and would be common to all nuclear generators, weight penalties for these components are not included in Table 7-2. Generator dose rates are summarized for current and near-future plutonia fuel forms. The indicated dose rates are generally acceptable for unmanned missions without further shielding, if no dose rate measuring instrumentation is present in close vicinity of the generator. If this instrumentation were present, additional exclusion distance or shadow shielding would be required.

ADVANCED TECHNOLOGY REVIEW

Growth potential of the multicell generator system is illustrated in Figure 7-6 where system specific power is plotted against generator power.

70-1148

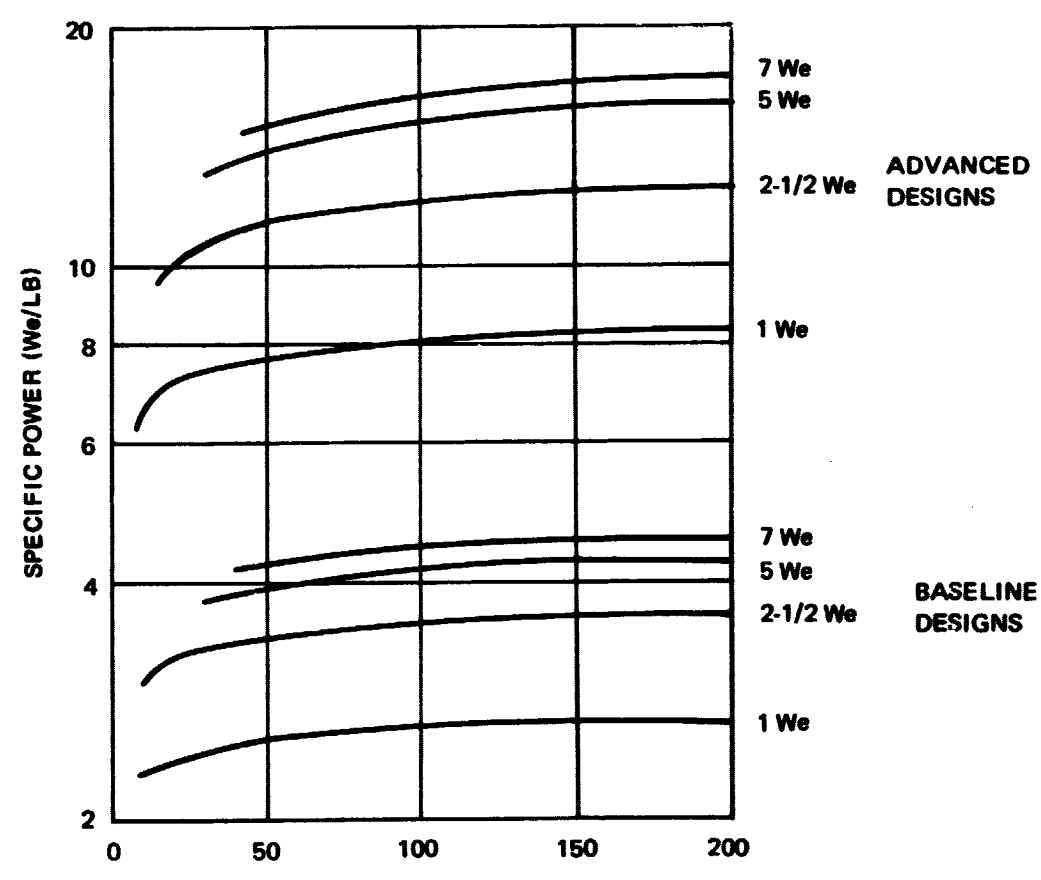

Figure 7-6. System Specific Powers for Optimum Stacking Options of Selected Cell Powers

The advanced technology design is characterized by spherical vented emitter capsules in place of cylindrical capsules, curia fuel in place of plutonia SSC, and W-O-Cs electrode surfaces in place of Ta-based surface systems. For the comparison shown, 1-mil electrode spacing and conventional aeroshell design is retained. The advanced-technology system becomes more compact than the baseline design, and, it is therefore probable, that the conventional aeroshell is an arbitrary constraint on system growth potential. The combination of advanced-technology components indicates future system specific power and conversion efficiency from 15 to 17 w_e/lb and 9% to 10%, respectively.

For each module power size, the continuum between the baseline and advanced designs may be reached by single technology improvements, not necessarily in combination with all others. The development of a curia fuel form, for instance, without improvement of any other parameter would double the potential specific power of the baseline design.

Section 8
CONCLUSIONS AND RECOMMENDATIONS

All objectives of the Phase I design study have been satisfied. The Isomite multicell space power generator has been shown to provide a highly flexible and redundant modular power supply satisfying space power requirements in the 50 to 200 w_e range with negligible compromise of system requirements. A basic building block module power of 5 w_e is identified for three generators with rated EOL power of 50, 100, and 200 w_e, respectively. The feasibility of a wide range of generators using a single basic module has tremendous economic benefit, both in the development and qualification program stages. Using the basic 5 w_e converter module, generators above 100 w_e have practically constant specific power of 4 w_e/lb with an overall conversion efficiency allowing for both design margin and system integration losses in excess of 6.5%. At generator power levels below 100 w_e, the inherently smaller number of modules per generator require a larger design margin to provide an acceptable confidence level for the EOL rated power. Inclusion of design margin in the lower generator power range reduces system performance to approximately 3.1 w_e/lb and 6% conversion efficiency.

The Phase I study has identified that there is no optimum voltage for the multicell generator at any generator power in the range of interest. Generator voltage is increased at the expense of systems specific power for all module/generator combinations considered. A two-column series-parallel connected converter network was found to provide adequate generator reliability consistent with an economically viable development and qualification program. Generators at each power level studied can be arranged with output from 3 to 10 v. Off-optimum design of converter parameters is available to compensate for system integration problems (for example: the match between T_c and T_{rad}).

The use of unvented cylindrical capsule technology was found to be a significant penalty on the multicell system. It is therefore recommended that only vented fuel capsule designs be considered in the Phase II effort.

It is recommended that the Phase II effort continue the design study based on the current technology component combination defined in Section 3. While the curium system has long-term growth potential, it is premature to invoke this technology for a systems study which emphasizes near term design credibility.

Although the spherical capsule has a significant specific power advantage, cylindrical geometry represents the majority of practical devices demonstrated by DWDL and has a technological base which allows the earliest development of converter components for the multicell generator. On the same basis, it would be premature to propose designs based on W-O-Cs surfaces in place of the Ta-based electrode system.

The Phase II study approach will identify fine-structure interactions of the converter and aeroshell system which have not been fully explored in the parametric Phase I study. The thermal balance of the converter array will be optimized with respect to system requirements in preference to achievement of maximum output from an individual converter. In this manner, tradeoffs which establish optimum system design in response to system imposed constraints will be evaluated.

Both the Phase I and Phase II studies neglect the potential advantage of using emitter thermal flux concentration to achieve converter designs at high Q/A values. The reliability of an Isomite converter array in a three dimensional three or more column network is also of interest. It is recommended that the design study be expanded to cover these important areas of potential benefit.

Section 9
NEW TECHNOLOGY

No new technology items have been reported to date. Computer programs, materials data, and construction techniques utilized in this study were available at DWDL prior to start of this contract.

PRECEDING PAGE BLANK NOT FILMED.

Section 10
REFERENCES

1. E. W. Williams and R. C. Howard. Development of a 100-W_e Isotope Thermionic Electrical Power Module. Proc. 2nd International Conference on Thermionic Electrical Power Generation, Stresa, Italy, May 1968.

2. Radio Corporation of America. Final Technical Report--The Development of Thermionic Isotope Space Power Technology (Volume 1, 2, and Appendix II - Classified Confidential, Appendix I - Unclassied. Contract NASw-1254, 1967.

3. J. G. DeSteese and J. S. Holmgren. A Radiantly Heated Radioisotope-Powered Thermionic Generator. Proc. Thermionic Conversion Specialist Conference, Palo Alto, California, October 1967.

4. R. L. Ryan and J. W. Graham. Isotope Reentry Vehicle Design Study. Preliminary Design Phase II - Final Report. NASA-CR-72555, August 1969.

5. AiResearch Manufacturing Div. Study of Radioisotope Fueled Brayton Cycle Electric Power System for MORL. M-1800 August 29, 1964 - Classified Confidential.

6. Donald W. Douglas Laboratories. Preliminary Design Study of a 250 W_e Promethium-147 Radioisotope Space Power System. DAC-59999, September 1967.

7. I. Langmuir. The Effect of Space Charge and Initial Velocities on the Potential Distribution and Thermionic Current Between Parallel Plane Electrodes. Physical Review, Vol. XXI, No. 4, 419, April 1923.

8. P. A. Lindsay and F. W. Parker. Potential Distribution Between Two Emitting Electrodes II. Thermionic Engines. J. Electronics and Control, Vol. 9, No. 2, 81, August 1960.

9. N. S. Rasor and E. E. Warner. Correlation of Emission Processes for Adsorbed Alkali Films on Metal Surfaces. J. Appl. Phys. Vol. 35, No. 9, 2589, September 1964.

10. B. A. Khrustalev and A. M. Rakov. Radiative Properties of Tantalum, Niobium, Graphite and Niobium Carbide at High Temperatures. Heat Transfer-Soviet Research. Vol. 1, No. 4, July 1969.

11. Y. S. Touloukian. Thermophysical Properties of High Temperature Solid Materials. Vol. 1 Elements, MacMillan 1967.

12. T. M. Houston and H. F. Webster. Advances in Electronics and Electron Physics. 17, 147, 1962.

13. C. G. Suits. The Collected Works of Irving Langmuir. Vol. 3, pages 285, 311, and 321, Macmillan 1961.

14. J. Leary. Passout for Isotope Fuels and Materials Committee Meeting, Oak Ridge National Laboratory, February 25-26, 1970.

15. W. M. Pardue, et al. Final Report for the Program to Develop Composite Fuel Forms of $Pu^{238}O_2$. BMI-1869, September 1969.

16. J. D. Watrous. DWDL Private Communication.

17. J. W. Holland and D. L. Bosseau. Thermionic Converter Network Reliability. General Atomic (John Jay Hopkins Laboratory) Report GA-6102, written for the Bureau of Ships, Department of the Navy, San Diego, California, March 19, 1965.

18. J. R. Long. Output Power Characteristics of Thermionic Converter Arrays Under Partial Failure Conditions. Advances in Energy Conversion Engineering, 1967 Intersociety Energy Conversion Engineering Conference, August 13-17, 1967, Miami Beach, Florida, pp. 163-170.

19. K. Shimada and F. de Winter. Optimization of Thermionic Generator Systems of High Reliability. Fifth Space Congress, Cocoa Beach, Florida, March 1968.

20. A. W. Barsell. Safety Analysis Report for a 4-Watt ^{147}Pm Isomite Miniature Radioisotope Thermionic Converter. MDAC Report DAC-60771 (October 1968).

21. M. W. Hulin. Radioisotope Heater Development Program. MDAC Report DAC-63364 or NASA-CR-101840, June 1969.

22. Hittman Associates, Inc. Spherical Capsule Technology Program. Heat Source Technical Report. HIT-370, January 1969.

23. D. F. Haskell. Impact Failure Criterion for Cylindrical and Spherical Shells. The Shock and Vibration Bulletin 39, Part 5 (December 1968).

24. A. W. Barsell and T. H. Smith. Optimum Configurations for Reentry Safety of 5 to 50 Wth Radioisotope Heaters. MDAC Paper WD 1343, to be presented at 16th Annual ANS Meeting, June 28 - July 2, 1970, Los Angeles, California.

25. D. W. Larson. Ablation and Thermal Analysis of the Apollo Lunar Radioisotope Heater. SC-RR-69-303, July 1969.